

Application of wavelet-artificial intelligence hybrid models for water quality prediction: a case study in Aji-Chay River, Iran

Rahim Barzegar¹ · Jan Adamowski² · Asghar Asghari Moghaddam¹

Published online: 18 January 2016
© Springer-Verlag Berlin Heidelberg 2016

Abstract The accuracy of Artificial Neural Network (ANN), Adaptive Neuro-Fuzzy Inference System (ANFIS), wavelet-ANN and wavelet-ANFIS in predicting monthly water salinity levels of northwest Iran's Aji-Chay River was assessed. The models were calibrated, validated and tested using different subsets of monthly records (October 1983 to September 2011) of individual solute (Ca^{2+} , Mg^{2+} , Na^+ , SO_4^{2-} and Cl^-) concentrations (input parameters, meq L⁻¹), and electrical conductivity-based salinity levels (output parameter, $\mu\text{S cm}^{-1}$), collected by the East Azarbaijan regional water authority. Based on the statistical criteria of coefficient of determination (R^2), normalized root mean square error (NRMSE), Nash–Sutcliffe efficiency coefficient (NSC) and threshold statistics (TS) the ANFIS model was found to outperform the ANN model. To develop coupled wavelet-AI models, the original observed data series was decomposed into sub-time series using Daubechies, Symlet or Haar mother wavelets of different lengths (order), each implemented at three levels. To predict salinity input parameter series were used as input variables in different wavelet order/level-AI model combinations. Hybrid wavelet-ANFIS ($R^2 = 0.9967$, NRMSE = 2.9×10^{-5} and NSC = 0.9951) and wavelet-ANN ($R^2 = 0.996$, NRMSE = 3.77×10^{-5} and NSC = 0.9946) models implementing the db4 mother wavelet decomposition outperformed the ANFIS

($R^2 = 0.9954$, NRMSE = 3.77×10^{-5} and NSC = 0.9914) and ANN ($R^2 = 0.9936$, NRMSE = 3.99×10^{-5} and NSC = 0.9903) models.

Keywords Water quality prediction · Artificial intelligence models · Discrete wavelet transform · Aji-Chay River · Iran

1 Introduction

As well as affecting local climate, river water serves as an important source of drinking water and groundwater recharge (Adamowski et al. 2010; Emamgholizadeh et al. 2014). Given the strong dependence of surface water quality (*i.e.*, its chemical, physical, and biological characteristics) on the nature and extent of agricultural, industrial and other anthropogenic activities within a region's catchments (Singh et al. 2009; Najah et al. 2013; Haidary et al. 2013), it is essential that, under typical development scenarios implemented in water quality modelling, its prediction be accurate. Such accuracy is key to enabling a river water quality manager to choose the management option that best meets a large number of identified goals (Palani et al. 2008; Emamgholizadeh et al. 2014).

A number of rather complex and data-intensive statistical and mathematical water quality models have been developed to enable potential water quality conservation best management practices to be chosen and tested for their efficacy (Einax et al. 1999). While statistical models, usually based on linear correlations between parameters and their attendant correlation coefficients, have a number of advantages over mathematical models, they are weak in handling nonlinear inter-parameter relationships (Campisi et al. 2012; Tiwari and Adamowski 2014, 2015). Artificial neural networks

✉ Jan Adamowski
jan.adamowski@mcgill.ca

¹ Department of Earth Sciences, University of Tabriz, 29 Bahman Boulevard, Tabriz, Iran

² Department of Bioresource Engineering, McGill University, 2111 Lakeshore Rd., Sainte-Anne-de-Bellevue, QC H9X3V9, Canada

(ANN) and adaptive neuro-fuzzy inference systems (ANFIS) are among the artificial intelligence modelling methods developed to address data nonlinearity (Nayak et al. 2004; Partal and Kiş 2007; Adamowski et al. 2012b; Yeniguna and Ecer 2012; Nourani et al. 2014; Belayneh et al. 2014; Karran et al. 2014; Rathinasamy et al. 2013, 2015). The loss of efficiency in handling data which occurs as the number and complexity of data sets for training of an ANN or ANFIS increases can be addressed through different data preprocessing approaches (Hadad et al. 2011). Wavelet analysis, one of the most important and useful of such approaches, offers multiresolution decomposition of a function into separate components (e.g., time, space, or frequency), thereby improving the analysis (Akansu and Haddad 1992; Adamowski et al. 2009; Nalley et al. 2012, 2013; Pingale et al. 2014; Araghi et al. 2015). Derived from Fourier transform analysis, wavelet analysis can be combined with a wide range of artificial intelligence modelling methods (e.g., Anctil and Tape 2004; Cannas et al. 2006; Kisi 2008; Adamowski and Sun 2010; Adamowski and Chan 2011; Nourani et al. 2011; Adamowski et al. 2012a; Kisi and Shiri 2012; Moosavi et al. 2013).

A number of studies have investigated the prediction of water quality parameters using artificial intelligence models such as ANN and ANFIS models. An ANN model was used to predict electric conductivity (EC) and dissolved oxygen (DO) for the Mamasin dam reservoir in central Turkey (Elhatip and Kömür 2008), as well as DO and biological oxygen demand (BOD) in India's Gomti River (Singh et al. 2009). Various water quality parameters of Malaysia's Johor River, including DO, EC, total dissolved solids (TDS) and turbidity, were predicted by ANN (Najah et al. 2011, 2013), ANFIS (Najah et al. 2012), or both ANN and ANFIS (Najah et al. 2014). Similarly, a comparison was made of both ANN and ANFIS models' ability to predict DO, BOD and chemical oxygen demand (COD) in Iran's Karoon River (Emamgholizadeh et al. 2014). Ghavidel and Montaseri (2014) used ANNs and two different ANFIS—one with grid partition and one with subtractive clustering—to predict TDS in Iran's Zarinehroud basin.

Given wavelet analysis' relatively recent entry into the domain of hydrology and water resources research, few studies have been conducted on the prediction of water quality parameters using wavelets. Using an integrated wavelet-ANFIS model with cross-validation and only considering an orthogonal wavelet prediction method for monthly water quality parameters (e.g., TDS, EC and turbidity), Najah et al. (2012), found the greatest accuracy to have been obtained by making the length of cross-validation one-fifth that of the data records. Moreover, they found that, in terms of predictive accuracy, the wavelet-ANFIS model outperformed the ANFIS model. Seeking to predict short-term water quality (i.e., DO) of intensive freshwater pearl

breeding ponds in Duchang County (Jiangxi Province, China), Xu and Liu (2013) showed that a Morlet-wavelet-based wavelet-ANN, while accurate, also proved to be faster, provided greater accuracy, and was more robust than either a BP neural network or an Elman neural network. Parmar and Bhardwaj (2015), seeking to predict the COD of India's Yamuna River using a wavelet neuro-fuzzy model implementing only 2nd to 8th order Daubechies wavelets, found that the series decomposed with an 8th order wavelet gave the best results for 9-month-ahead prediction. Ravan-salar and Rajaee (2015) applied artificial neural network (ANN) and wavelet-neural network hybrid (WANN) models, based on monthly period discharge (Q) and EC of the current and previous periods as inputs to the models, to predict one month ahead EC of the Asi River at the Demirköprü gauging station, Turkey. They concluded that the performance of the proposed WANN model was better than that of the conventional ANN model.

In order to improve ANN and ANFIS models' performance in predicting water salinity, expressed in terms of conductance (EC, in $\mu\text{S cm}^{-1}$), the present study coupled such models with wavelet transformations implementing wavelets of different orders (*i.e.*, wavelet length) within different wavelet families [*e.g.*, Daubechies (db), Symlet (sym) or Haar]. The performance of the wavelet-AI models thus generated was compared with respect to how accurately models enhanced with wavelets of different orders and families predicted water salinity.

2 Methods

2.1 Artificial neural network models

The artificial neural network (ANN) employs, as the name implies, a model structure which mimics a human neural network. A very powerful computational technique for modeling complex non-linear relationships, particularly in situations where the explicit form of the relationship between the variables involved is unknown (Smith 1994; Singh et al. 2009), it identifies and learns the patterns of correlation between input and objective values. Its network is comprised of interconnected nodes or neurons (Parmar and Bhardwaj 2015). The Multi-Layer Perceptron (MLP) type of ANN consists of three layers: (i) the input layer, where the data are introduced to the network, (ii) one or more hidden layer(s), where the data are processed and, (iii) an output layer, where the results for given inputs are produced (Junsawang et al. 2007; Cho et al. 2011). In a three layer feed-forward perceptron ANN (Fig. 1), nodal data are multiplied by weights to compute the signal strength, and then are transferred to the next node in the network; the input layer nodes accept the input vectors and forward the

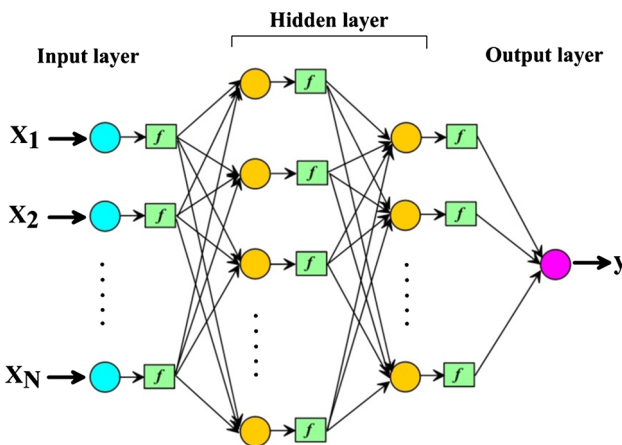


Fig. 1 Structure of a three-layer feed forward perceptron ANN

signals to the next layer according to the connection. This process is continued until the signals reach the output layer. Multi-layer networks use a variety of learning techniques. Back-propagation is the most commonly used training algorithm in multilayer feed-forward networks.

2.2 Adaptive neuro-fuzzy inference system

The adaptive neuro fuzzy inference system (ANFIS) was introduced by Jang (1993) as a neural network functionally equivalent to a Sugeno type inference model. ANFIS uses a feed-forward network to search for fuzzy decision rules that perform well on a given task. Using a given input-output data set, ANFIS creates an FIS for which membership function parameters are adjusted using either a back propagation algorithm alone or a combination of a back propagation algorithm and a least-squares method (Abdulshahed et al. 2015). This allows the fuzzy systems to learn from the data being modeled.

The equivalent ANFIS architecture of the Sugeno inference system (Fig. 2) consists of five layers, and the relationship between the input and output of each layer is summarized as follows:

- Layer 1: Every node i in this layer is an adaptive node with a node output, O , defined by:

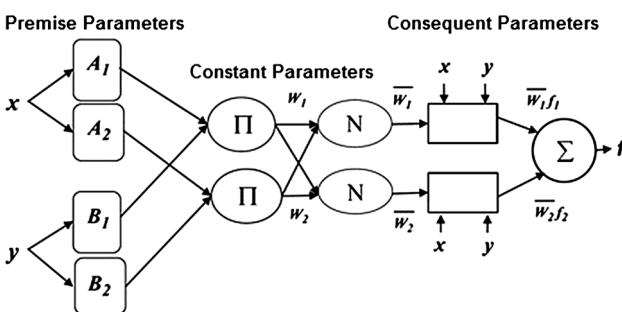


Fig. 2 A typical ANFIS architecture (Jang 1993)

$$\begin{aligned} O_{1,i} &= \mu_{A_i}(x) \quad \text{for } i = 1, 2, \text{ or} \\ O_{1,i} &= \mu_{B_{i-2}}(y) \quad \text{for } i = 3, 4 \end{aligned} \quad (1)$$

where x (or y) is the input to the node, and A_i (or B_{i-2}) is a fuzzy set associated with this node, and characterized by the shape of the node's membership function (μ). This function must be continuous and piecewise differentiable, such as, for example, a Gaussian function. If such is used as a membership function, $\mu_{A_i}(x)$ can be computed as:

Parameters in this layer are referred to as premise (antecedent) parameters.

- Layer 2: Every node in this layer is a fixed node labeled as Π , which multiplies the incoming signals and output product. For instance,

$$\mu_{A_i}(x) = e^{-\frac{1}{2}\left(\frac{x-C_i}{\sigma_i}\right)^2} \quad (2)$$

where $\{\sigma_i, c_i\}$ are parameter sets.

- Layer 3: Every node in this layer is a circular node labeled as N . The i th node calculates the ratio of the i th rule's firing strength to the sum of all rules' firing strengths.

$$O_{2,i} = w_i = \mu_{A_i}(x) \times \mu_{B_i}(y) \quad i = 1, 2 \quad (3)$$

with each output node representing the firing strength of a rule.

$$O_{3,i} = \bar{w} = \frac{w_i}{w_1 + w_2} \quad i = 1, 2 \quad (4)$$

This layer's outputs are termed normalized firing strengths.

- Layer 4: Node i in this layer computes the contribution of the i th rule towards the model output, with the following node function:

$$O_{4,i} = \bar{w}_i f_i = \bar{w}_i (p_i x + q_i y + r_i) \quad (5)$$

where w_i is the output of Layer 3 and $\{p_i, q_i, r_i\}$ is the parameter set. Parameters in this layer are referred to as consequent parameters.

- Layer 5: The single node in this layer is a fixed node, labeled P , that computes the overall output as the summation of all incoming signals.

$$O_{5,i} = \sum_{i=1}^{i=2} \bar{w}_i f_i = \frac{\sum_{i=1}^{i=2} w_i f_i}{\sum_{i=1}^{i=2} w_i} \quad (6)$$

2.3 Wavelet transform (WT)

Various mathematical transforms have been developed to draw out information not immediately or easily available from raw signals. The basic aim of wavelet analysis is to

both determine the frequency (or scale) content of a signal and to assess the temporal variation of this frequency content. In this method, the data series are broken down by transformation into its ‘wavelets’, a scaled and shifted version of the mother wavelet (Grossmann and Morlet 1984). The wavelet transform (WT) is a relatively recent and very precise method for signal and time series processing (Hernández and Weiss 1996; Torrence and Compo 1998; Percival and Walden 2000; Nievergelt 2001; Olkkonen 2011; Kirchgässner et al. 2013). While the general theory behind WT is quite similar to that of short time Fourier transform (STFT), WT allows for a completely flexible window function (called the mother wavelet), which can be changed over time based on the shape and compactness of the signal (Nievergelt 2001; Percival and Walden 2000). Developed within the mathematics community during the last two decades, WT analysis appears to be a more effective tool than Fourier Transform (FT) in studying nonstationary time series (Partal and Kişi 2007). Given this property, WT can be used to analyze the time–frequency characteristics of any kind of signal or time series. Continuous wavelet transform (CWT) of a signal $f(t)$ is a time-scale technique of signal processing that can be defined as the integral of the full signal over the entire period, multiplied by scaled, shifted versions of the wavelet function $\psi(t)$, given mathematically as (Lau and Weng 1995; Mallat 1998; Partal and Kişi 2007; Adamowski and Chan 2011):

$$W_x(a, b, \psi) = \frac{1}{\sqrt{a}} \int_{-\infty}^{+\infty} f(t) \psi^* \left(\frac{t-b}{a} \right) dt \quad (7)$$

where $\psi(t)$ represents the mother wavelet function, a is the scale index parameter (*i.e.*, inverse of the frequency), and b is the time shifting parameter, also known as translation.

A discrete wavelet transform (DWT) can therefore be derived by discretizing Eq. (7), where a and b are two parameters given as follows:

$$a = a_0^m, \quad b = n a_0^m b_0 \quad (8)$$

where the variables n and m are integers that control the wavelet dilation and translation, respectively. a_0 is the specified dilation step greater than 1; and b_0 is the location parameter, which must be greater than zero (Mallat 1998). Substituting a and b in Eq. (7) results in (Grossmann and Morlet 1984; Mallat 1998):

$$W_x(a, b, \psi) = a_0^{-m/2} \int_{-\infty}^{+\infty} f(t) \psi^* \left(a_0^{-m} t - nb_0 \right) dt \quad (9)$$

namely the mathematical relationship of the DWT.

Compared to the classical CWT, which requires a significant amount of computation time and data (Adamowski 2008; Partal and Kişi 2007), the DWT requires less computation time and is simpler to develop. The DWT scales and positions are usually based on powers of two (dyadic scales and positions) (Christopoulou et al. 2002).

2.4 Model performance comparison

In this study, four different statistical performance evaluation criteria are used for comparing the model output results to measured values. These include the coefficient of determination (R^2), normalized root mean square error (NRMSE), Nash–Sutcliffe efficiency coefficient (NSC) and threshold statistics (TS). The coefficient of determination (R^2) measures the degree of correlation between the observed and predicted values. R^2 values range from 0 to 1, with 1 indicating a perfect relationship between the data and the line drawn through them, and 0 representing no statistical correlation between the observed and predicted data. The Normalized Root Mean Square Error (NRMSE) is the ratio of the root mean square error to the natural variance of the observed variable (σ^2). A value of $NRMSE = 0$ indicates perfect prediction while a value of $NRMSE = 1$ corresponds to a prediction of the statistical average. The Nash–Sutcliffe model efficiency coefficient (NSC) can also be used to assess the prediction power of hydrological models. The Nash–Sutcliffe efficiencies can range from $-\infty$ to 1. An efficiency of one ($NSC = 1$) corresponds to a perfect match of predicted data to the observed data. An efficiency of zero ($NSC = 0$) indicates that the model predictions are as accurate as the mean of the observed data, whereas an efficiency less than zero ($NSC < 0$) occurs when the observed mean is a better predictor than the model.

$$R^2 = \frac{\left(\sum_{i=1}^N (P_i - \bar{P})(O_i - \bar{O}) \right)^2}{\left(\sum_{i=1}^N (P_i - \bar{P})^2 (O_i - \bar{O})^2 \right)} \quad (10)$$

$$NRMSE = \frac{\left(\frac{1}{N} \sum_{i=1}^N (P_i - O_i)^2 \right)^{1/2}}{\sigma^2} \quad (11)$$

$$NSC = 1 - \frac{\sum_{i=1}^N (O_i - P_i)^2}{\sum_{i=1}^N (O_i - \bar{O})^2} \quad (12)$$

where N is the number of observations, O_i is the i th observed value, P_i is the i th predicted value, \bar{P} and \bar{O} are the mean values of P_i and O_i , respectively, and σ is the standard deviation of the observed values.

Since these criteria show the magnitude of a model’s error but do not provide any information on error distribution, to test the robustness of the network’s output, it is

important to test the model using other performance evaluation criteria such as threshold statistics (TS) (Jain and Indurthy 2003; Noori et al. 2009; Kant et al. 2013). The TS gives a performance index not only in terms of predicting a variable but also with respect to the distribution of prediction errors. The TS for a level of $x\%$ is a measure of the consistency in prediction errors from a particular model. The TS is represented as TS_x , and is expressed as a percentage. This criterion can be expressed for different levels of absolute relative error (ARE) from the model. ARE is given as:

$$ARE = \left| \frac{O_i - P_i}{O_i} \right| \quad (13)$$

For the ARE, the threshold statistics (TS_x) computed for the $x\%$ level are:

$$TS_x = \frac{Y_x}{n} \times 100 \quad (14)$$

where Y_x is the number of the salinity prediction (out of n total computed) for which the ARE is less than $x\%$ from the model.

3 Study area and data

3.1 Study area

The Aji-Chay River watershed (lat. $37^{\circ}24'–38^{\circ}3.7'N$, and long. $45^{\circ}30'–47^{\circ}45'E$) is located in northwest Iran's East Azarbaijan province, east of Lake Urmia (Fig. 3). This watershed is under the influence of middle-latitude westerlies, with most of the rain occurring over the region originating from depressions moving over the area after forming over the Mediterranean Sea and travelling on a branch of the polar jet stream in the upper troposphere (Asghri Moghaddam and Allaf Najib 2006; Barzegar et al. 2015b). The annual mean temperature in the study area is about $12.8^{\circ}C$, ranging from $35^{\circ}C$ in the summer to below zero in the winter when cold fronts move through the area.

The Aji-Chay River extends about 276 km to the Lake Urmia Delta, with its watershed covering about 13853 km^2 . The Aji-Chay River, a major source for recharge of local aquifers (e.g., Tabriz plain aquifer), carries high levels of sediment and salinity and flows in a roughly northeast-southwest direction. The river's main source of salinity, the Upper Red Formation (Miocene series), widely exposed in the north-eastern part of the Tabriz region, consists of red marls with gypsum, conglomerate, salt and marly limestone (Barzegar 2014; Barzegar et al. 2015a). Due to its very low gradient, the Aji-Chay River divides into a multi-branched delta and eventually discharges, at the end of the Tabriz plain, to Lake Urmia, the second saltiest lake in the world (Barzegar et al. 2015a). The river is fed by melting snow of

the Bozgoush, Sahand and Arasbaran mountain ranges. In recent years, the Tabriz region has been faced with an environmental crisis due to the dumping of industrial and urban sewage into the Aji-Chay River (Barzegar 2014).

3.2 Data

Given its importance in terms of the Aji-Chay River's water quality, salinity [EC ($\mu\text{S cm}^{-1}$)] was chosen as the water quality parameter of interest. The physicochemical parameters of flow rate, electrical conductivity (EC), pH, Temperature, and concentrations of Ca^{2+} , Mg^{2+} , Na^+ , K^+ , HCO_3^- , CO_3^{2-} , SO_4^{2-} and Cl^- were assessed (Table 1), for Aji-Chay River water samples collected monthly by the East Azarbaijan regional water authority over the period of October 1983–September 2011 at the Akhula hydrometric station, situated near the river Delta and connected to Lake Urmia (Fig. 3).

One of the most important steps in developing a prediction model is the selection of the input variables. To select input parameters for the models being developed, variables related to EC on the basis of strong Pearson correlations were used, while those parameters with weak correlations to EC were ignored (Table 2). The parameters used as inputs were the concentrations of Ca^{2+} , Mg^{2+} , Na^+ , SO_4^{2-} and Cl^- , while the output was EC. The input–output data were divided into a calibration set (October 1983 to December 2003); validation set (January 2004 to December 2008) and testing set (January 2009 to September 2011).

Variance-based sensitivity analysis was used to investigate the effects of the input variables on the model output. Variance-based sensitivity analysis can be performed with the correlation ratio (Borgonovo and Plischke 2015). As the input/output relationship is linear, the correlation ratio is tantamount to the square of the Pearson correlation coefficient. Sensitivity analysis showed that the most important input is Na^+ concentration because it has the highest Pearson correlation coefficient: $r(\text{Na}^+, \text{EC}) = 0.983$ indicating that this input alone explains $(0.983)^2 \times 100 = 96.62\%$ of the output variance and that its contribution is linear. The Cl^- concentration was the second most important input but was also correlated with Na^+ , such that its effect was embedded in the effect of Na^+ . Note that the remaining 3.38 % of the output variance may be due to error noise.

To speed up the model calibration process, data were normalized to an interval by transformation of means:

$$X_N = \frac{X - X_{min}}{X_{max} - X_{min}} \quad (15)$$

where X_N is the normalized value of variable X , and $0 \leq X_N \leq 1$, while X_{max} and X_{min} are, respectively, the

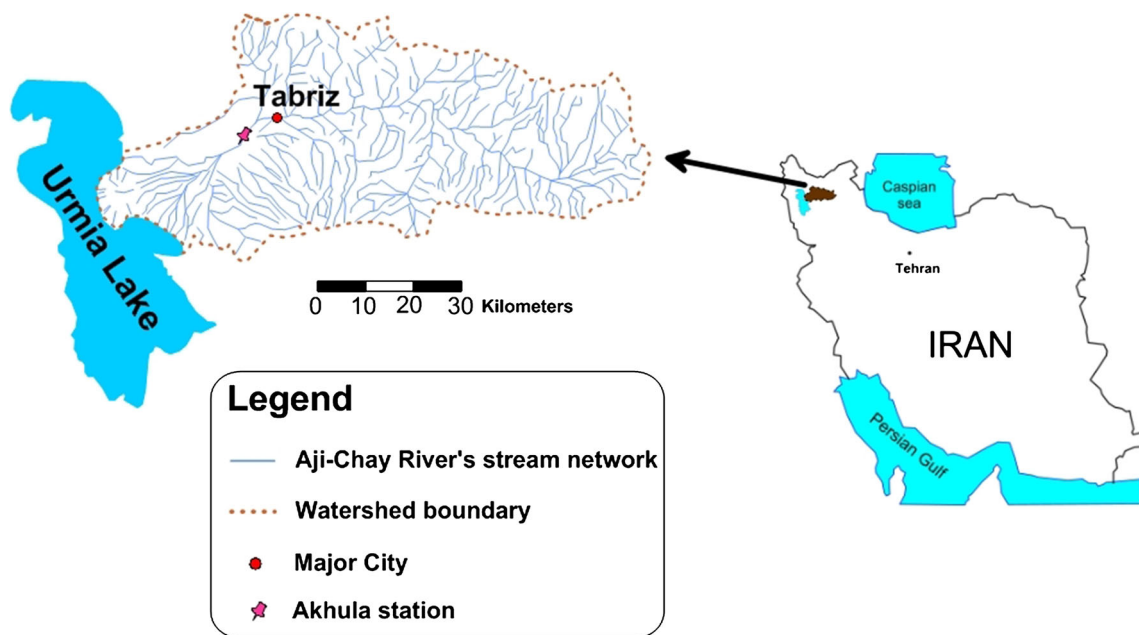


Fig. 3 Aji-Chay River watershed and location of the Akhula station

Table 1 Flow rate and measured physicochemical water parameters in Aji-Chay River water, ($n = 336$)

	Flow rate	pH	Temp.	EC	Na^+	K^+	Ca^{2+}	Mg^{2+}	CO_3^{2-}	HCO_3^-	SO_4^{2-}	Cl^-
Unit	$\text{m}^3 \text{ day}^{-1}$	–	$^\circ\text{C}$	$\mu\text{S cm}^{-1}$	meq L^{-1}							
Min	0.1	6.5	10	1500	5.4	0.06	2	0.8	0	1	3	7.6
Max	138.47	8.9	23	28,000	230	1.2	26	33	0.5	11.5	80.3	237.5
Median	1.72	7.5	18	6050.5	47	0.34	8.73	6.22	0	4.99	7.95	47.5
Mean	9.95	7.49	17.59	6928.93	53.08	0.379	9.24	6.96	0.018	5.08	11.69	53.46
SD	20.51	0.41	3.8	4090.82	34.97	0.22	4.39	4.22	0.077	1.57	12.19	35.43
Variance	420.76	0.17	14.47	1.6×10^7	1223	0.052	19.3	17.82	0.006	2.48	148.69	1256

Table 2 Pearson correlation to determine best input parameters for the models

	Flow rate	Temp.	pH	EC	Na^+	K^+	Mg^{2+}	Ca^{2+}	CO_3^{2-}	HCO_3^-	SO_4^{2-}	Cl^-	
Flow rate	1												
Temp.	-0.158	1											
pH	-0.023	0.071	1										
EC	-0.371	0.202	-0.157	1									
Na^+	-0.353	0.301	-0.132	0.983	1								
K^+	-0.080	-0.012	-0.081	0.034	0.042	1							
Mg^{2+}	-0.309	0.272	-0.140	0.782	0.731	0.136	1						
Ca^{2+}	-0.361	0.237	-0.237	0.798	0.733	-0.010	0.692	1					
CO_3^{2-}	-0.085	0.046	0.559	0.002	0.014	-0.009	-0.019	-0.085	1				
HCO_3^-	-0.374	0.022	0.237	0.181	0.180	0.124	0.073	0.195	-0.032	1			
SO_4^{2-}	-0.190	0.214	-0.128	0.756	0.764	0.051	0.643	0.504	0.057	0.007	1		
Cl^-	-0.357	0.314	-0.172	0.965	0.948	0.032	0.757	0.795	-0.022	0.168	0.591	1	

maximum and minimum value of variable X of the original data.

The models' training completed, normalized model outputs were denormalized to actual values:

$$X = [X_N(X_{max} - X_{min})] + X_{min} \quad (16)$$

4 Model development

4.1 ANN and ANFIS models

Two artificial intelligence (AI) models, an ANN and an ANFIS, were developed for prediction of salinity. The major steps for development of ANN models include defining the suitable model inputs, specifying network type, pre-processing and partitioning of the available data, determining network architecture, defining model performance criteria, calibration (optimization of connection weights), and validation of the model (Govindaraju 2000; Maier and Dandy 2000; Dawson and Wilby 2001). Feed-forward neural networks are among the most common neural networks in use (Mehrotra et al. 1997) and were chosen for use in this particular study because they are simple, easily trained, and can be readily inverted.

To develop a three-layered ANN model, four inputs were used in the first layer. Given that trial and error is well documented to be an appropriate way to determine the best number of neurons in the hidden layer (Mishra and Desai 2006; Rahimikhoob 2010; Moosavi et al. 2013; Shirmohammadi et al. 2013), this method was employed. The number of neurons in the hidden layer was three and in the output layer one neuron was included for EC data. The three-layered ANN was trained using the Levenberg–Marquardt training algorithm (TrainLM). The transfer function between layer one and layer two was TANSIG, while PURELIN was employed for the last layer. The magnitude of the gradient and the number of validation checks used to terminate network training are presented in Fig. 4a. At an epoch of 15 iterations, the gradient was 1.0389×10^{-4} , barely above the 1×10^{-4} threshold below which training will stop, and at six the validation checks also indicated training should stop. The performance plot (Fig. 4b) shows the value of the function, in terms of calibration, validation, and testing behaviors, versus the iteration number. The best validation performance, based on the mean square error, was 2.8656×10^{-4} at epoch 9. When the training of the model was completed, the testing data served as model input and salinity values were predicted.

The ANFIS model was calibrated and tested using the same data sets as those used for the ANN model. A hybrid algorithm combining the least-squares method and the back

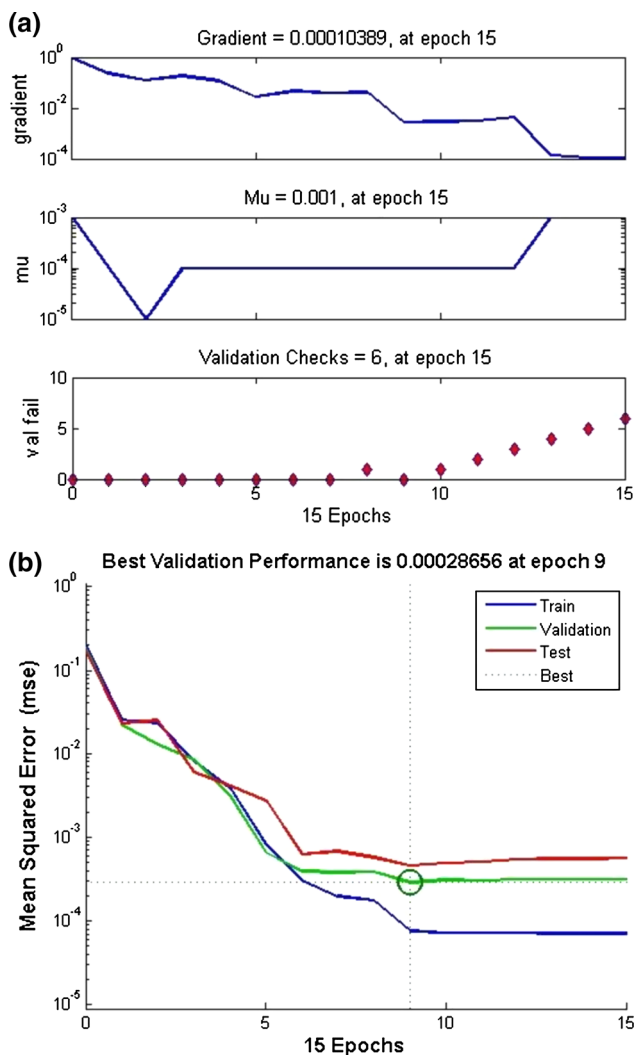


Fig. 4 Training state and performance of the MLP neural network model developed

propagation gradient descent method was applied to optimize and adjust the Gaussian membership function parameters and coefficients of the output linear equations (Zounemat-Kermani and Teshnehlab 2008; Fijani et al. 2013). In this study, the Gaussian membership function was used because it generated the least error in the fuzzification of the data collected for the components. The number of epochs and error tolerance were set to 500 and 0, respectively. Subtractive fuzzy clustering, based on a measure of the density of data points in the feature space (Chiu 1994), was used to establish the rule-based relationship between the input and output variables. The best ANFIS model performance was achieved when the clustering radius was set to 0.5 and the number of fuzzy rules was 2. Two Gaussian membership functions were extracted for the ANFIS model's input variables (Fig. 5). After 2 epochs of training no further improvement was found in the

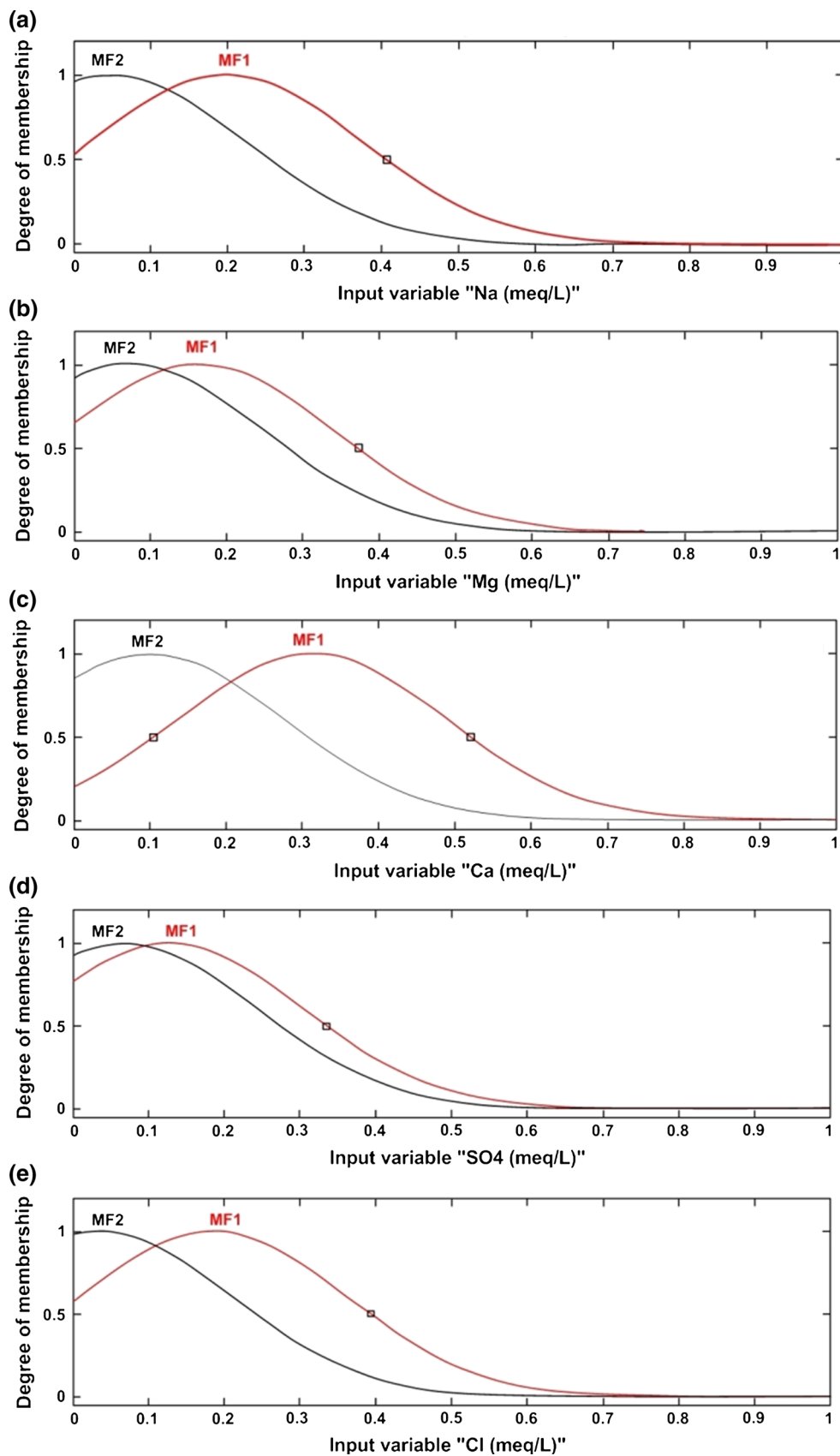
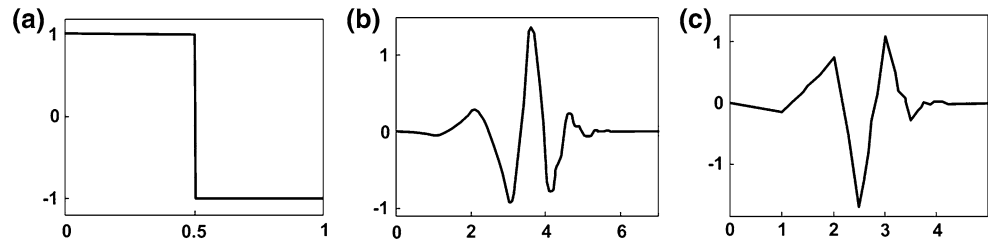


Fig. 5 Sugeno-FIS generated Gaussian membership functions for **a** Na^+ , **b** Mg^{2+} , **c** Ca^{2+} , **d** SO_4^{2-} and **e** Cl^- concentration data

Fig. 6 **a** Haar wavelet, **b** Daubechies-4 (db4) wavelet, and **c** Symlet-3 (Sym3) wavelet



performance of the model and training was stopped. The trained ANFIS model was tested with 33 samples not used in the calibration step.

4.2 Hybrid wavelet-ANN and wavelet-ANFIS models

In order to build hybrid wavelet-ANN and wavelet-ANFIS models, in a first step the original data (*i.e.*, Ca^{2+} , Mg^{2+} , Na^+ , SO_4^{2-} and Cl^- concentrations and EC) were decomposed into the sub-series components of details (*i.e.*, detailed frequency and time series of the input data) and approximations of the sub-series using a discrete wavelet transformation (DWT). The original time series was decomposed into lower resolution components by iterating the decomposition of successive approximation signals. In a second step, all sub-series parameters were summed to then serve as ANN or ANFIS model inputs.

Before performing wavelet decomposition, three model parameter aspects needed to be selected: the mother wavelet, its order, and the number of levels of decomposition. The choice of the mother wavelet depends on the data to be analyzed. In choosing the appropriate mother wavelet, its attributes and the characteristic of its signal should be carefully considered (Parmar and Bhardwaj 2015). Selection of an appropriate wavelet function poses significant challenges and is governed largely by the problem at hand and some of the distinctive properties of the wavelet function such as (i) its region of support, and (ii) the number of vanishing moments (Maheswaran and Khosa 2012b). The energy content of the Haar wavelet, for example, is concentrated over the narrowest support band and, therefore, has good localization properties and, therefore, makes it the most suitable for change detection studies (Ahuja et al. 2005). Moreover, Nourani et al. (2011, 2013, 2014) stated that similarity in shape between the mother wavelet and that of the time series under study is the best guideline in choosing the proper mother wavelet; therefore, it might be a useful idea to investigate similarities from another point of view than form (*e.g.*, energy). A more detailed discussion of the selection of wavelets for different time series is presented in Maheswaran and Khosa (2012a). In this study, Daubechies, Symlet and Haar mother wavelets were used based on similarity in shape

between these mother wavelets and the time series. Also, numbers of vanishing moments between 1 and 7 were tested.

Thus, in the present case observed data series were decomposed into sub-time series using the commonly employed Daubechies, Symlet and Haar mother wavelets of different lengths (*i.e.*, orders) (Nourani et al. 2009; Nalley et al. 2012, 2013; Rathinasamy et al. 2013). The function shape of the mother wavelets employed are shown in Fig. 6. Finally, the required number of decomposition levels, L , must be specified (Aussem et al. 1998; Nourani et al. 2009, 2014; Adamowski and Chan 2011; Tiwari and Chatterjee 2011; Moosavi et al. 2013):

$$L = \text{int}[\log(N)] \quad (17)$$

where N is the number of time series data. In this study, $N = 336$, so $L \approx 3$. Therefore, three wavelet decomposition levels were selected (D_1 , D_2 and D_3).

Plots of the wavelet decomposition series of input data series with the db4 wavelet (Figs. 7, 8, 9, 10, 11, 12) show lower detail levels to have higher frequencies and therefore represent the dataset's rapidly changing component, while higher detail levels have lower frequencies and therefore represent the dataset's slowly changing component. The approximation components (A_3) represent the slowest changing component of the dataset (including the trend).

Wavelet-AI models were separately tested for various input combinations of the decomposed time series and the output (predicted EC) was the summation of the outputs from each decomposed time series. Data series were divided into a calibration set (November 2002 to June 2008), a validation set (July 2008 to February 2009), and a testing set (March 2009 to October 2009) similar to the AI models.

To improve model accuracy, wavelet pre-processed data were used as ANN model inputs. The feed-forward ANN networks consisted of an input layer, three hidden layers, and a single output layer consisting of a single node denoting the water salinity. The input nodes consisted of various combinations of the discrete wavelet (DW) series (and the approximation series) of input data. For all models the optimum number of neurons was found to be 7. The three-layered ANN was trained using the Levenberg–Marquardt training algorithm (TrainLM) with the TANSIG and PURELIN transfer functions for layers one and two,

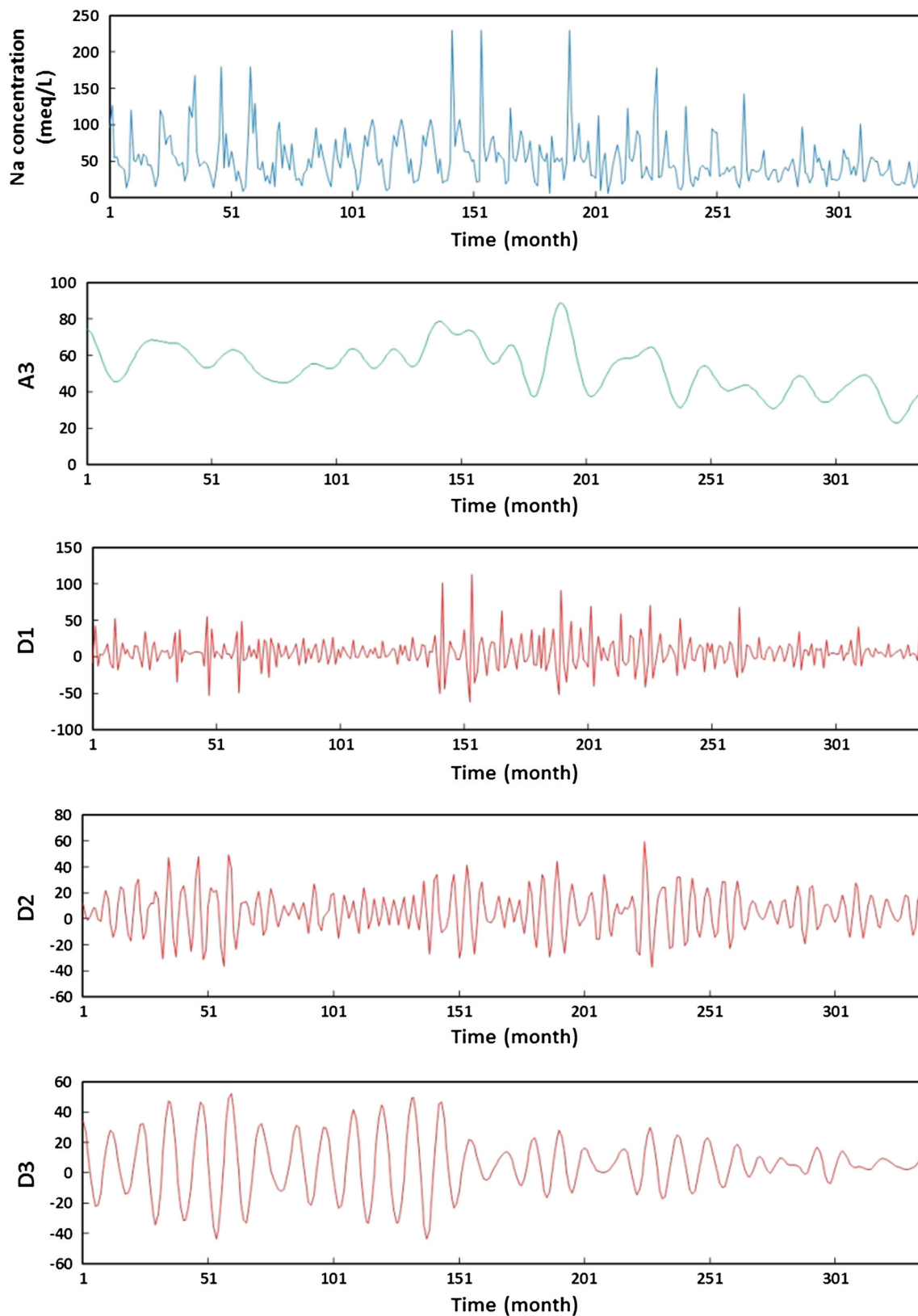


Fig. 7 Wavelet decomposition series of monthly Na^+ concentration data from Akhula station, using the db4 wavelet at level 3

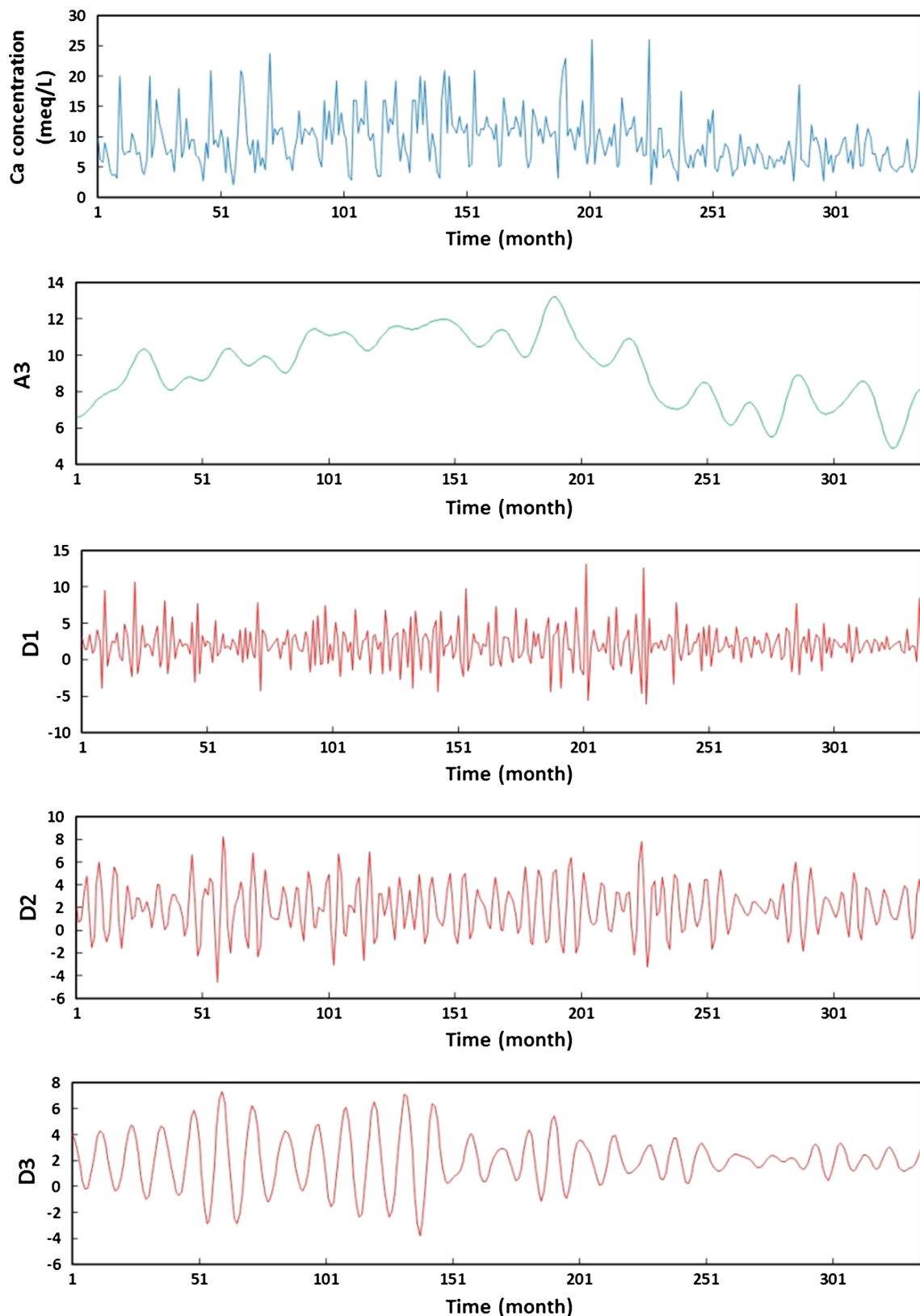


Fig. 8 Wavelet decomposition series of monthly Ca^{2+} concentration data from Akhula station, using the db4 wavelet at level 3

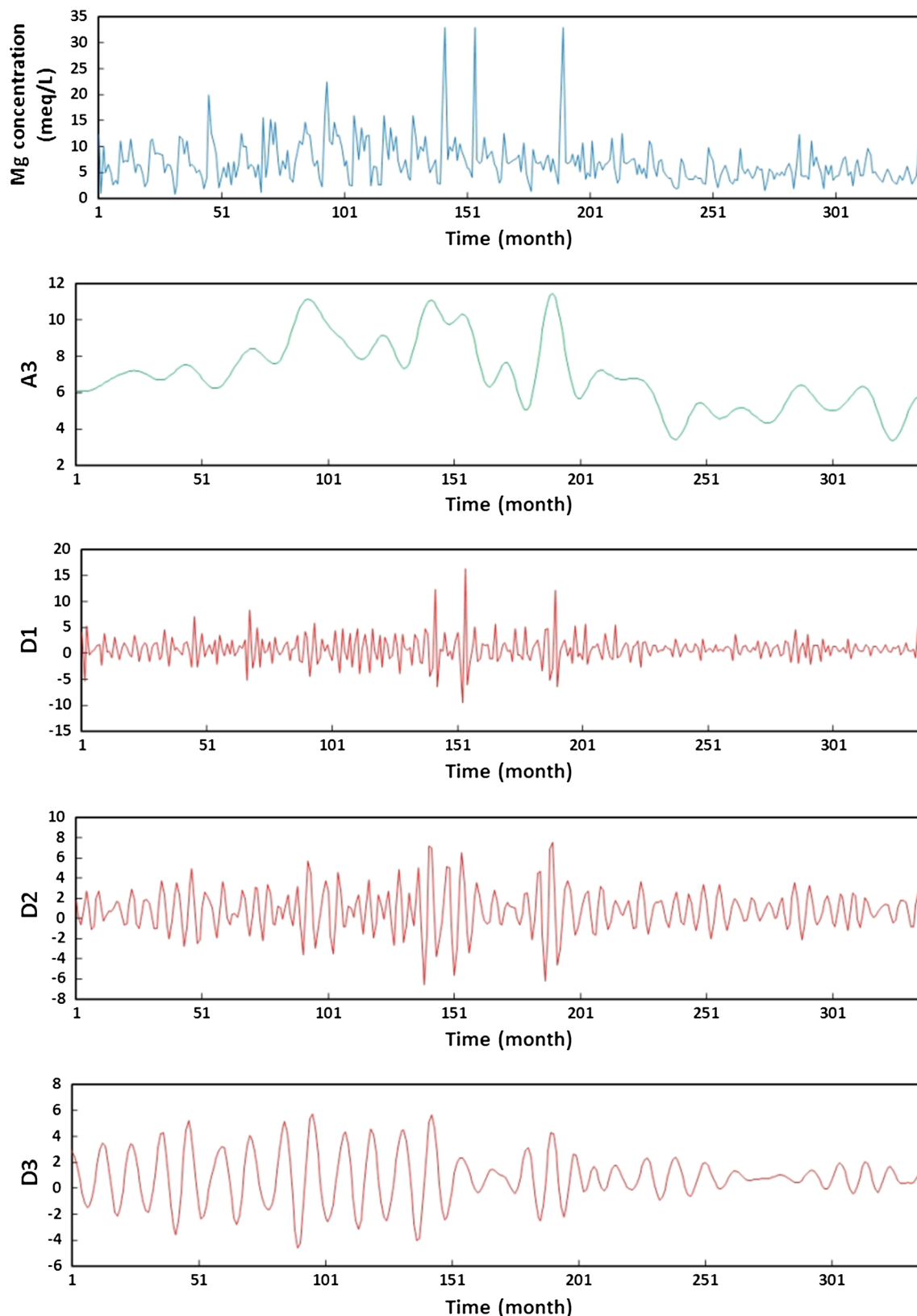


Fig. 9 Wavelet decomposition series of monthly Mg^{2+} concentration data from Akhula station, using the db4 wavelet at level 3

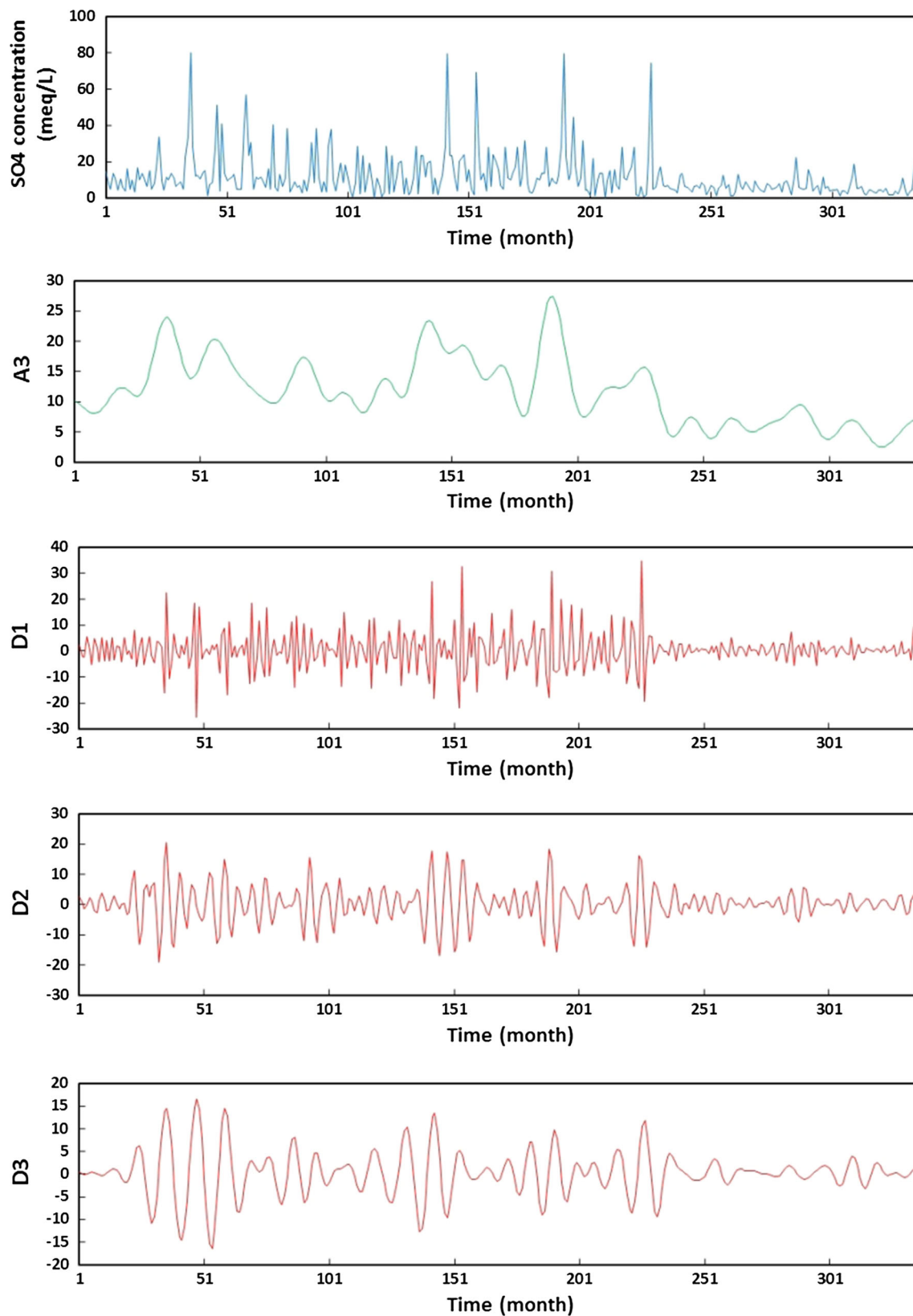


Fig. 10 Wavelet decomposition series of monthly SO_4^{2-} concentration data from Akhula station using the db4 wavelet at level 3

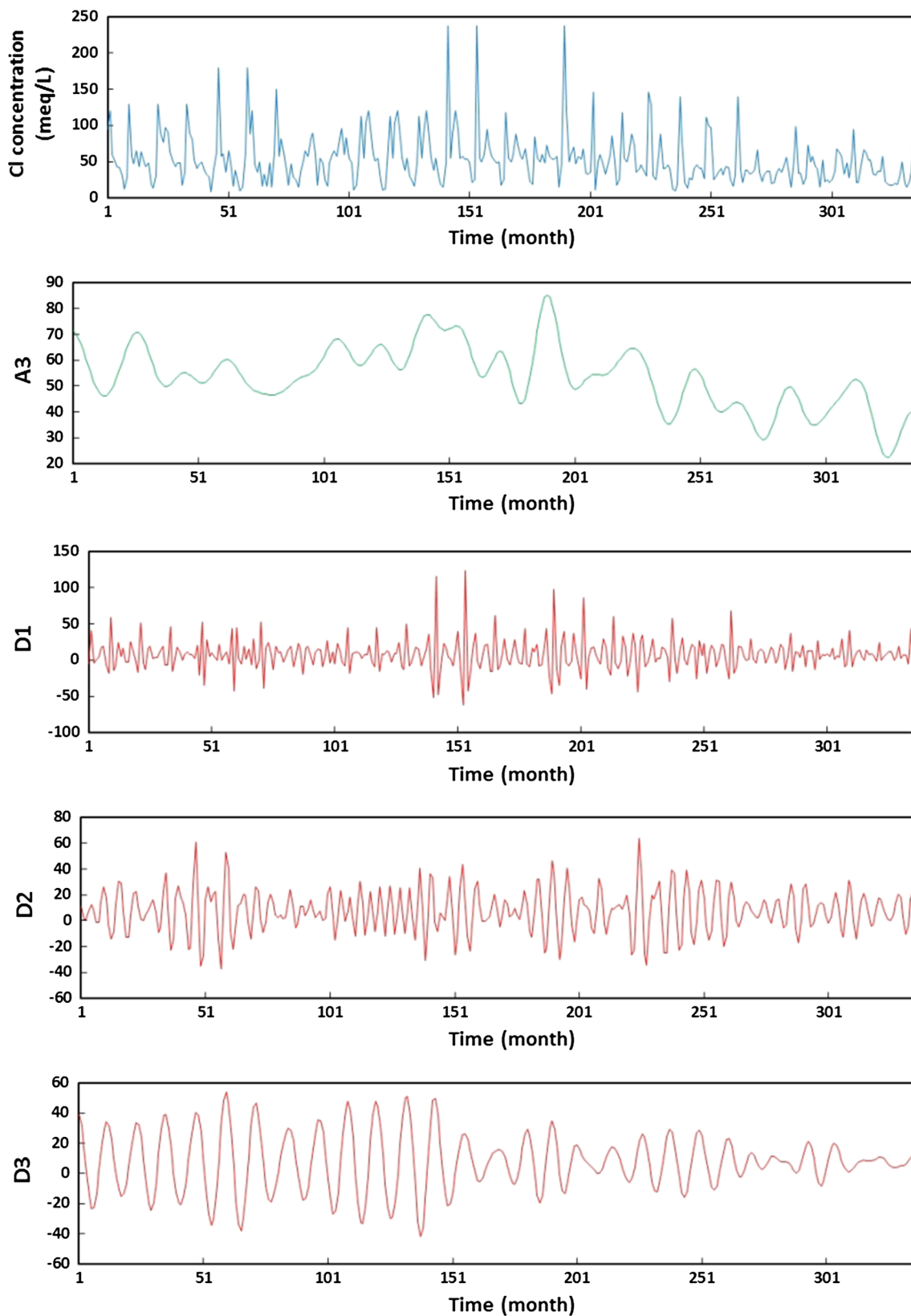


Fig. 11 Wavelet decomposition series of monthly Cl^- concentration data from Akhula station using the db4 wavelet at level 3

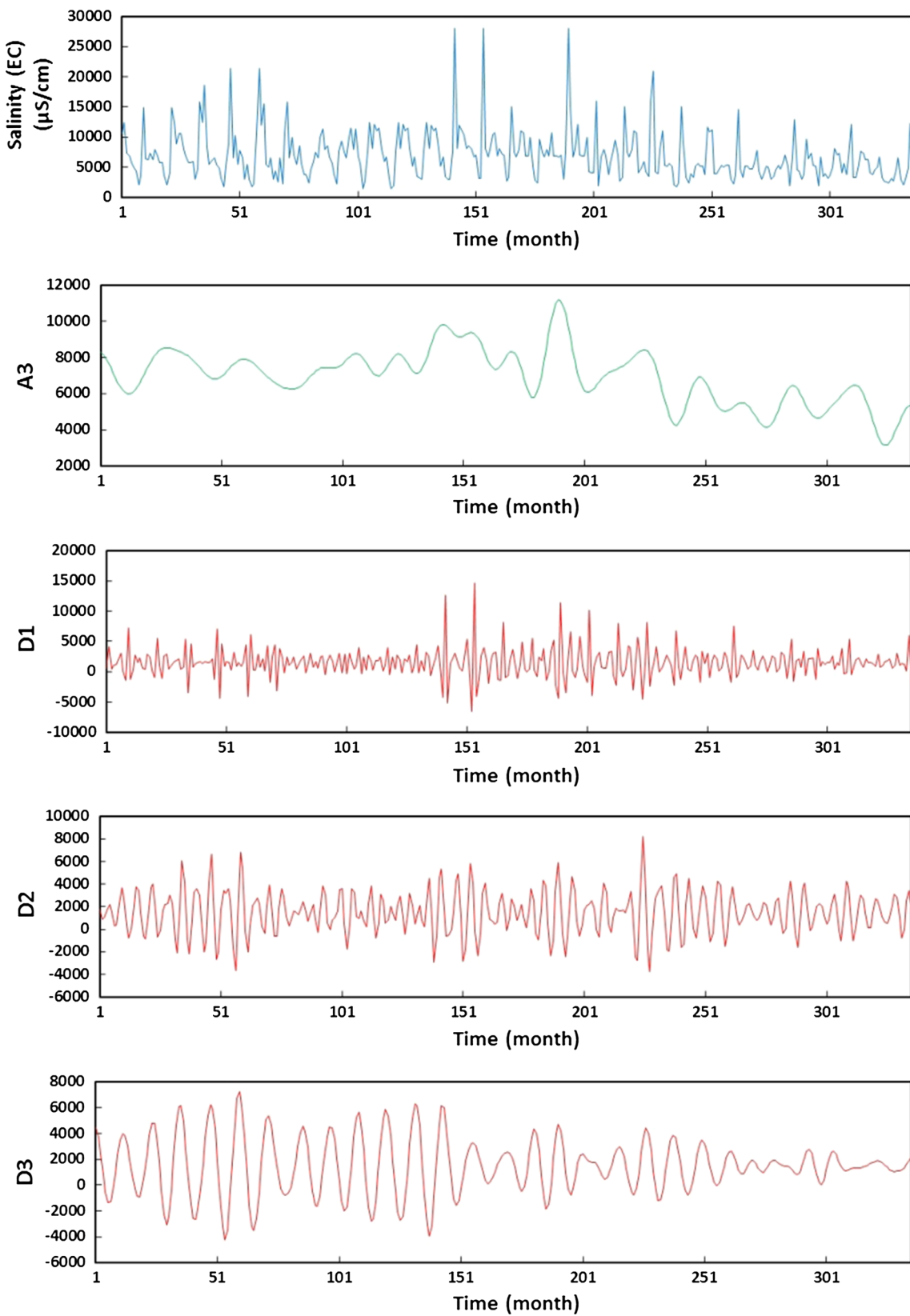


Fig. 12 Wavelet decomposition series of monthly salinity (expressed as electrical conductivity, $\mu\text{S cm}^{-1}$) data from Akhula station using the db4 wavelet at level 3

respectively. The networks thus generated were calibrated using the calibration data set, and after obtaining appropriately accurate results, the calibrated models were validated using the validation data set.

To construct the wavelet-ANFIS model, each decomposed time series was tested separately in the ANFIS models and the wavelet-ANFIS predicted output was simply obtained by summing the decomposed wavelets. A hybrid algorithm was applied to optimize and adjust the Gaussian membership function parameters in all ANFIS models. In the wavelet-ANFIS model for decomposition wavelets, both grid partitioning and subtractive clustering were used to generate FIS. For example, for decomposition wavelets with db4, the generated FIS for D_1 - and D_2 -decomposed time series were a grid partition with 32 rules, while for D_3 and A_3 subtractive clustering occurred with a clustering radius of 0.95 (with 2 rules) and 0.6 (with 4 rules), respectively. The results of predicted coefficients of decomposed time series with db4 for tested data are shown in Fig. 13.

5 Results

5.1 Artificial intelligence (AI) models

After training the proposed ANN model, the model was tested with 33 testing samples. The R^2 , NRMSE and NSC of the ANN model over the testing period were 0.9936, 3.99×10^{-5} and 0.9903, respectively. Observed and ANN-model-predicted salinity during the testing period are compared in Fig. 14.

The R^2 , NRMSE and NSC of the ANFIS model for the testing data were 0.9954, 3.77×10^{-5} and 0.9914, respectively (Table 3). Observed and ANFIS-model-predicted salinity during the testing period are compared in Fig. 15. For improved evaluation of the results via the use of TS, the distributions of the prediction errors for ANN and ANFIS are plotted (Fig. 16). This figure shows that ARE for 40 % of prediction of the testing stage in ANN and ANFIS are 1.55 and 1.7 %, respectively. However, ARE for 60 and 80 % prediction of the testing stage in ANN are 4.23 and 5.35 % and in ANFIS are equal to 3.46 and 5.35 %, respectively.

Generally, the ANFIS model performed better than the ANN model based on R^2 , NRMSE, NSC and TS, but the ANFIS shows a slope that differs more from 1, and an intercept that differs more from 0 than the ANN. This may be related to the effect of fuzzification of the input through membership functions. These results concur with those of Rajaei et al. (2009), Adamowski and Chan (2011), Nourani et al. (2011), Moosavi et al. (2013), Fijani et al. (2013),

Emamgholizadeh et al. (2014) and Parmar and Bhardwaj (2015).

5.2 Coupled wavelet-artificial-intelligence models

Based on their R^2 , NRMSE and NSC values, the wavelet-ANN models with db4 and db1 mother wavelets showed the best and worst performance, respectively (Table 4). The db mother wavelets (except db1) outperformed both the sym and Haar wavelets.

Figure 17 shows observed and wavelet-ANN-predicted EC over time. The R^2 , NRMSE and NSC for the linear relationship between observed and db4-mother-wavelet-ANN-predicted EC (Fig. 17) were 0.996, 3.43×10^{-5} and 0.9946, respectively. The distribution of the prediction error for wavelet-ANN models in the testing period is shown in Fig. 18. It can be seen that the TS for ARE less than 2 % is 51.5 and 30.3 % for the db4-mother-wavelet-ANN and db1-mother-wavelet-ANN, respectively. However, the TS for ARE less than 6 % is 84.8 and 93.9 % for the db4-mother-wavelet-ANN and db1-mother-wavelet-ANN, respectively.

Similarly to the wavelet-ANN models, wavelet-ANFIS model performance statistics (R^2 , NRMSE and NSC) for monthly salinity prediction indicate that the db4 and db1 mother wavelets showed the best and worst performance, respectively (Table 5). As with the wavelet-ANN models, the Haar actually shows better performance than all but db4.

Figure 19 shows observed and wavelet-ANFIS-predicted EC over time. For the testing period, the R^2 , NRMSE and NSC for the linear relationship between observed and db4-wavelet-ANFIS-predicted EC (Fig. 19) were 0.9967, 2.9×10^{-5} and 0.9951, respectively. The distribution of the prediction error for wavelet-ANFIS models in the testing period is shown in Fig. 20. It can be seen that the TS for ARE less than 2 % is 42.4 and 30.3 % for the db4-mother-wavelet-ANN and db1-mother-wavelet-ANN, respectively. However, the TS for ARE less than 6 % is 93.9 % for both the db4-mother-wavelet-ANN and db1-mother-wavelet-ANN models. In this study the NRMSE were more useful than R^2 and NSC in showing improvement in model performance. In the NRMSE criterion the errors are averaged after they are squared, so the NRMSE assigns a different weight to the errors (De Giorgi et al. 2015). Therefore, because of the weighting property of the NRMSE criteria, the difference between the predictions is greater than that observed through the R^2 and NSC.

The mother wavelet db4 is one of the wavelets of the Daubechies family which are called compactly supported orthonormal wavelets. Tables 3 and 4 show that the db4 wavelet function was the best mother wavelet for both models in the prediction of EC, and this may be because of

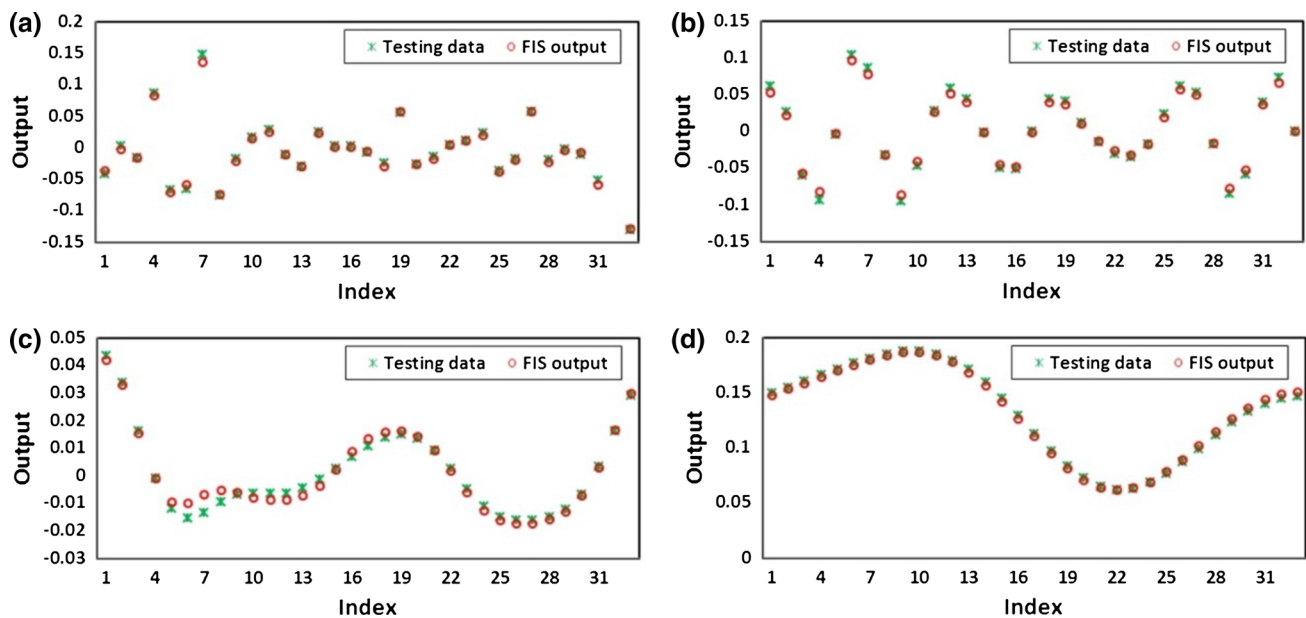
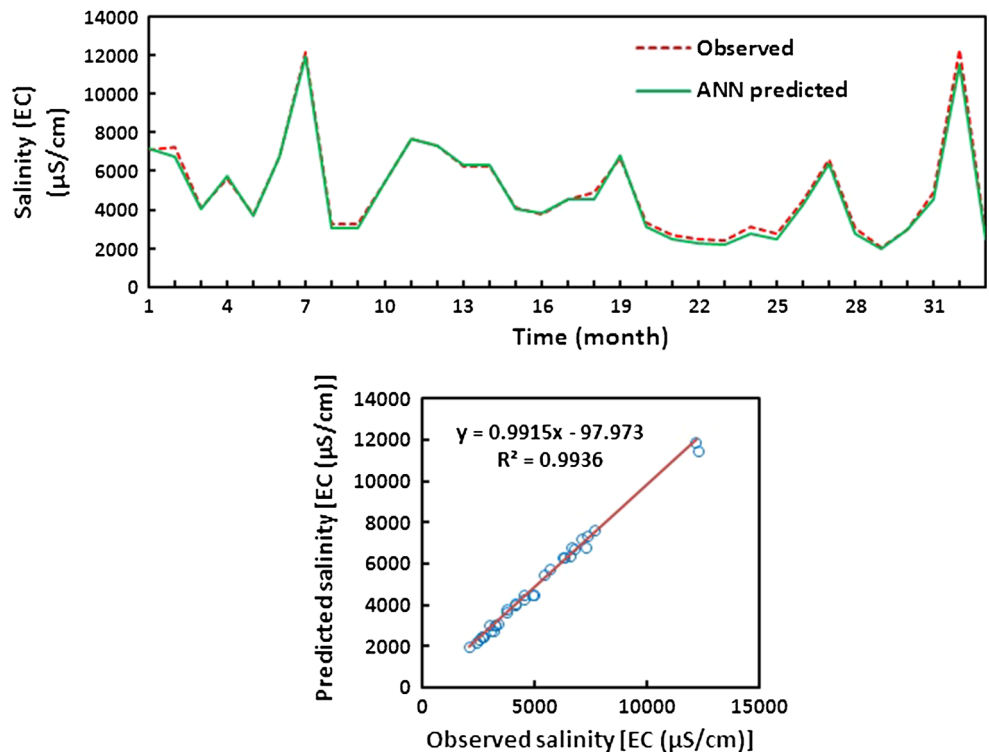


Fig. 13 The results of predicted coefficients of **a** D_1 , **b** D_2 , **c** D_3 and **d** A_3 decomposed time series with db4 wavelet between actual and tested results using a wavelet-ANFIS model

Fig. 14 Comparison of observed and predicted salinity [$\text{EC } (\mu\text{S cm}^{-1})$] for ANN model in testing period



the function shape (Fig. 6) of the db4 which is relatively similar to the salinity time series. Successful application of the db4 for non-stationary hydrologic data pre-processing has also been reported by Kisi (2008) and Nourani et al. (2009, 2011, 2013).

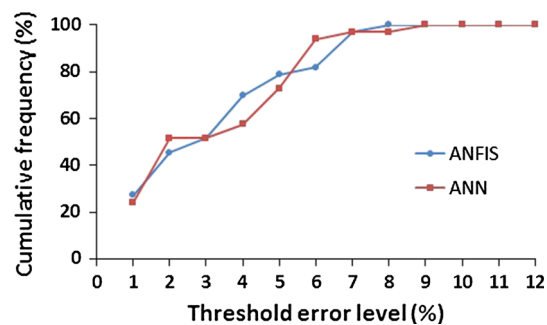
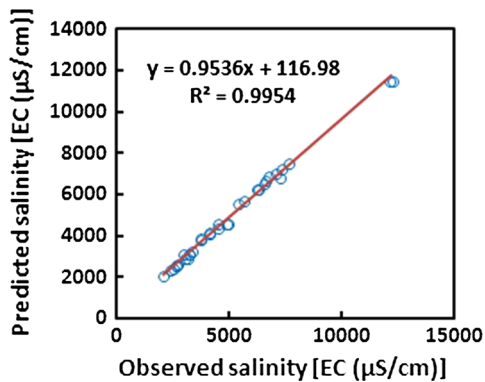
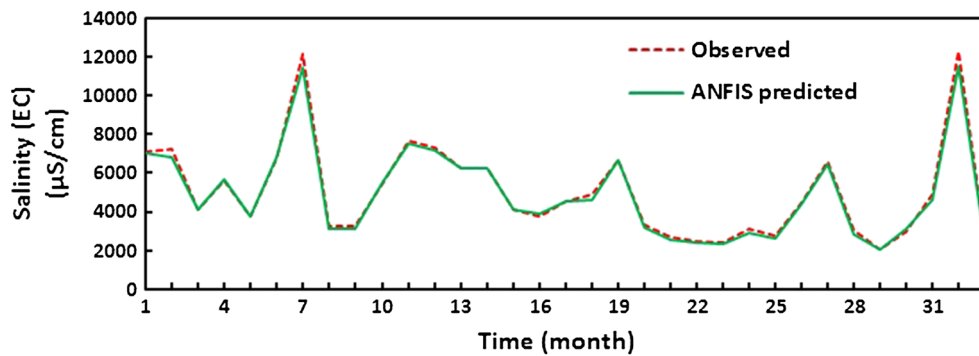
The db mother wavelets of different orders were not all able to provide good predictions: a lower order db wavelet (db1) gave poor model performance compared to models based on higher order wavelets such as db7 (Tables 4, 5). It can be seen that wavelets with high vanishing

Table 3 Accuracy of ANN and ANFIS models for prediction of Aji-Chay River salinity over the testing period

	R ²	NRMSE	NSC
ANN model	0.9936	3.99×10^{-5}	0.9903
ANFIS model	0.9954	3.77×10^{-5}	0.9914

moments can be helpful in increasing the reliability and performance of wavelet-artificial intelligence hybrid models (Sehgal et al. 2014). Model accuracy follows the order wavelet-ANFIS > wavelet-ANN > ANFIS > ANN, indicating that hybrid wavelet-ANFIS and wavelet-ANN models outperformed their respective conventional counterparts. The greater performance of the hybrid wavelet-ANN and wavelet-ANFIS models arose from the fact that these models can extract the characteristics and complex variations of the signals (*i.e.*, model inputs) precisely, by decomposing the non-stationary and complex signals into several stationary and simpler signals. Approximation coefficients denote the deterministic components, such as tendency/trend and period, whereas detail coefficients denote the stochastic components and noise. These stationary signals can highlight the fine structures and therefore, reduce the interference between the deterministic components and the stochastic components, thereby increasing the stability of the data variations.

The hybrid wavelet-AI models explored in this study demonstrate the advantage of using wavelets for improving

Fig. 15 Comparison of observed and predicted electrical conductivity for ANFIS model in testing period**Fig. 16** Distribution of prediction error for ANN and ANFIS models in the testing period

prediction accuracy. In this study, because of the high correlation of the inputs and output, the performance of the ANN, ANFIS, wavelet-ANN and wavelet-ANFIS models are almost similar. However, the wavelet-AI models do improve the accuracy of the predictions in comparison with single AI models.

6 Conclusions

This study employed Artificial Neural Network (ANN), Adaptive Neuro-Fuzzy Inference System (ANFIS), wavelet-ANN and wavelet-ANFIS models to predict Aji-Chay River (Iran) salinity, based on Ca^{2+} , Mg^{2+} , Na^+ , SO_4^{2-} and Cl^- concentrations. Aji-Chay River water quality data monitored over a period of 28 years were collected by the

Table 4 Accuracy of wavelet-ANN models using different db wavelets for prediction of Aji-Chay River salinity over the testing period

Mother wavelet	Decomposition level	R ²	NRMSE	NSC
db1	3	0.2583	2.25×10^{-3}	-33.64
db2	3	0.9924	4.66×10^{-5}	0.9868
db4	3	0.996	3.43×10^{-5}	0.9946
db5	3	0.9947	3.86×10^{-5}	0.9909
db7	3	0.9937	4.55×10^{-5}	0.9874
sym3	3	0.9783	6.15×10^{-5}	0.9771
sym4	3	0.9895	5.49×10^{-5}	0.9817
sym5	3	0.9889	6.61×10^{-5}	0.9734
Haar	3	0.9877	5.06×10^{-5}	0.9845

Fig. 17 Comparison of observed and predicted electrical conductivity for wavelet-ANN model with db4 mother wavelet at level 3 in testing period

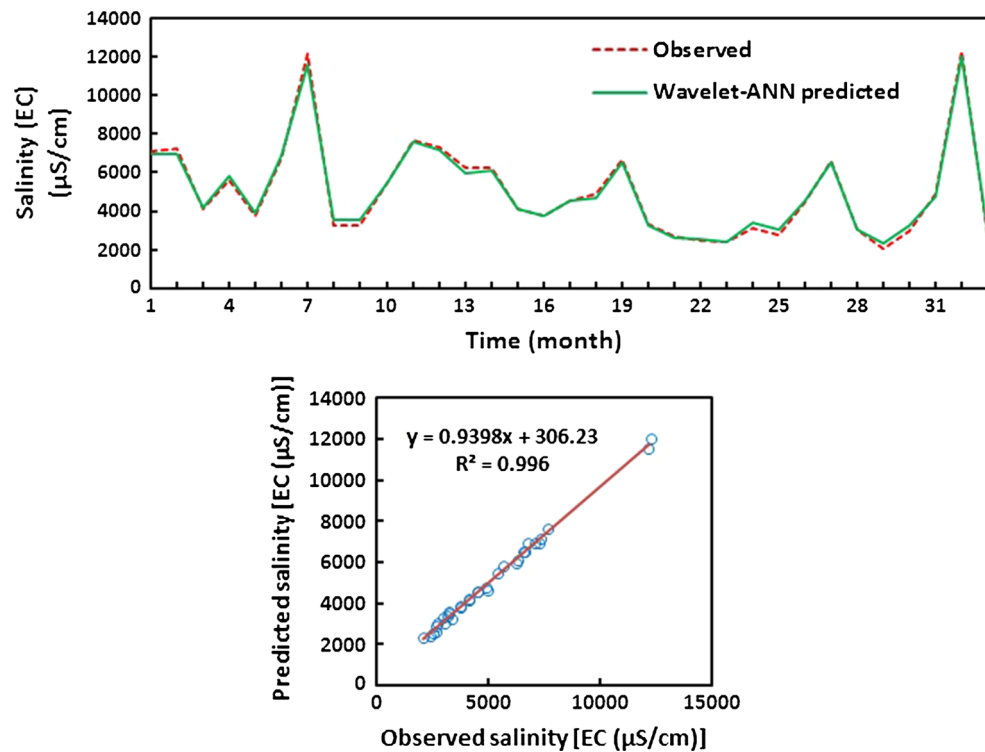


Fig. 18 Distribution of the prediction error for wavelet-ANN models in the testing period

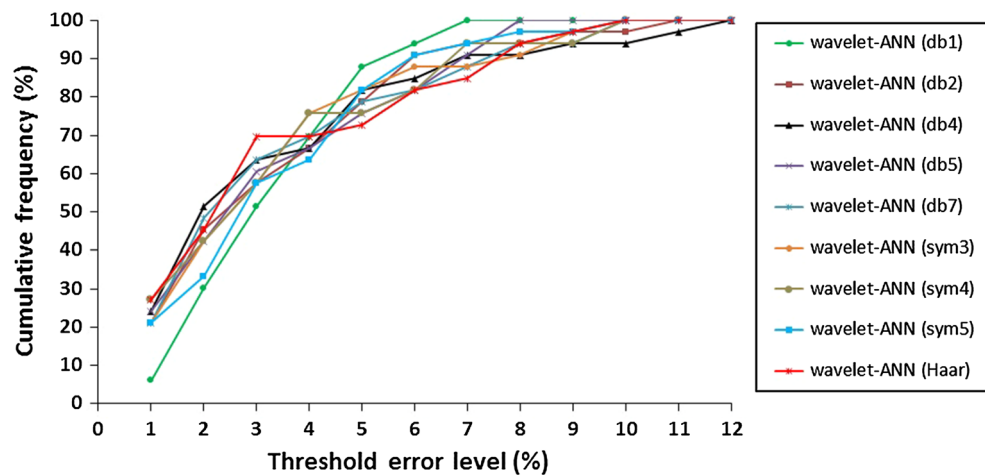


Table 5 Results of wavelet-ANFIS models using different mother wavelets (db, sym and Haar) for prediction of Aji-Chay River salinity over the testing period

Mother wavelet	Decomposition level	R ²	NRMSE	NSC
db1	3	0.2949	2.38×10^{-3}	-29.82
db2	3	0.9956	2.96×10^{-5}	0.9947
db4	3	0.9967	2.90×10^{-5}	0.9951
db5	3	0.9950	3.66×10^{-5}	0.9920
db7	3	0.9938	3.66×10^{-5}	0.9919
sym3	3	0.9925	4.02×10^{-5}	0.9902
sym4	3	0.9917	4.86×10^{-5}	0.9847
sym5	3	0.9905	4.86×10^{-5}	0.9857
Haar	3	0.9958	2.92×10^{-5}	0.9948

Fig. 19 Comparison of observed and predicted salinity [EC ($\mu\text{S cm}^{-1}$)] for db4-mother-wavelet-ANFIS model for the testing period

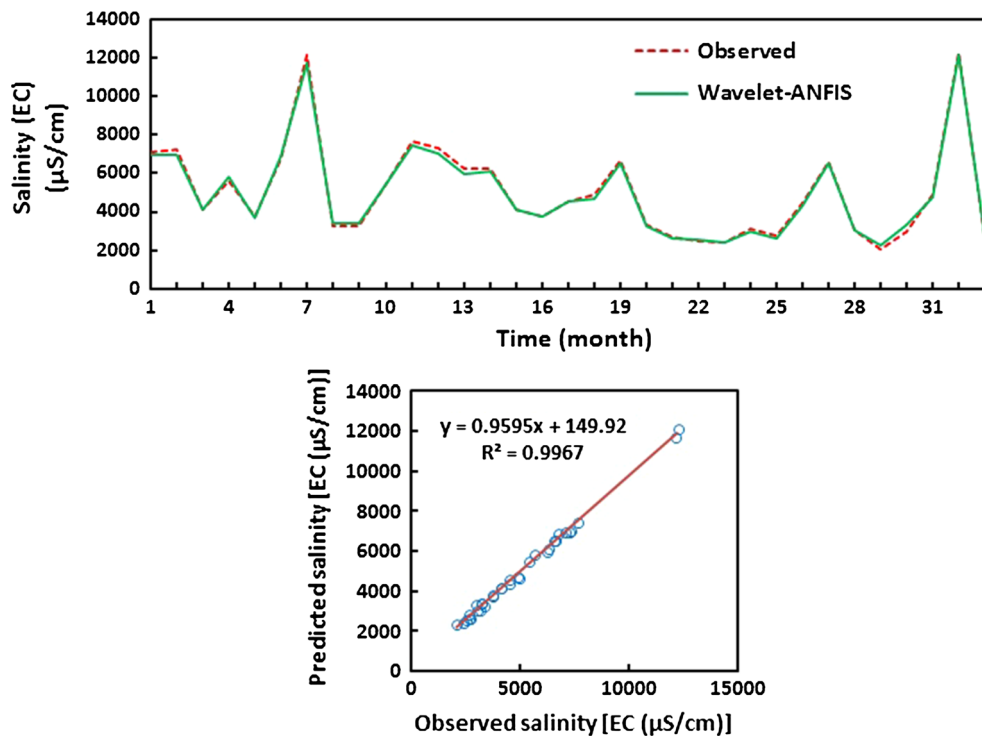
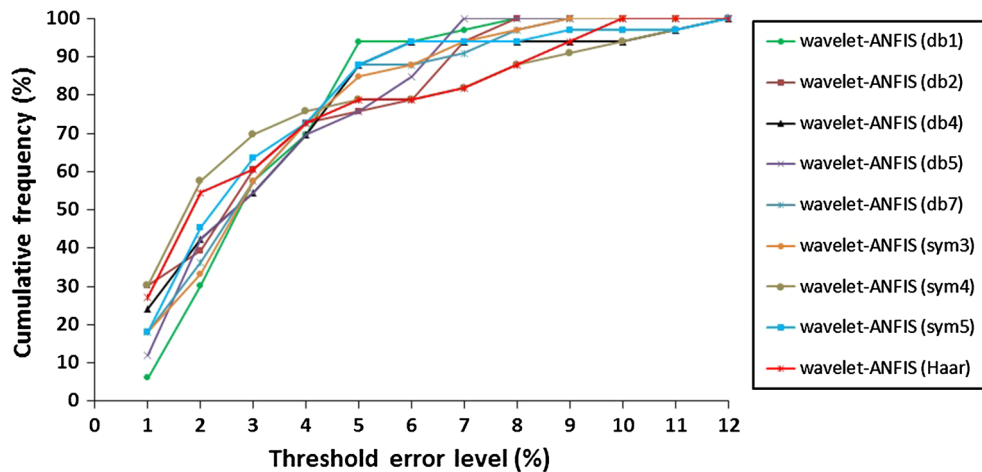


Fig. 20 Distribution of the prediction error for wavelet-ANFIS models in the testing period



East Azarbaijan regional water authority and served in the calibration, validation and testing of the models developed in this study. The coefficient of determination (R^2), normalized root mean square error (NRMSE), Nash–Sutcliffe efficiency coefficient (NSC) and threshold statistics (TS) were used to evaluate the models. In order to build the hybrid wavelet-ANN and wavelet-ANFIS models, the original data were decomposed into sub-series components using Daubechies, Symlet and Haar wavelets of different lengths (orders), at three levels. Then, all the parameters of the decomposed sub-series were used as inputs to the ANN or ANFIS models in order to develop hybrid wavelet-AI models. The ANN, ANFIS, wavelet-ANN and wavelet-ANFIS models were compared. In the testing phase, the R^2 , NRMSE and NSC for the wavelet-ANN model with db4 wavelets were 0.996, 3.77×10^{-5} and 0.9946, respectively, whereas those for the equivalent wavelet-ANFIS model were 0.9967, 2.9×10^{-5} and 0.9951, showing that the hybrid wavelet-ANFIS and wavelet-ANN models operating with the db4 mother wavelet performed better than the conventional ANFIS and ANN models. Also, the TS criteria showed good performance for the db4 mother wavelets. However, not all db mother wavelets were able to provide good predictions, depending on their order. It can be concluded that wavelets with high vanishing moments can be helpful in increasing the reliability and performance of wavelet-artificial intelligence hybrid models. The wavelet-ANFIS model was shown to outperform the wavelet-ANN model. This study showed that the ANN-based models in general showed good performance for water quality prediction when highly correlated inputs are used for salinity prediction. These types of new methods can be used to facilitate the transition to more sustainable water resources management (Saadat et al. 2011; Halbe et al. 2013, 2014; Koljinjvadi et al. 2014; Straith et al. 2014; Inam et al. 2015; Butler and Adamowski 2015).

Acknowledgments The authors would like to acknowledge the East Azarbaijan regional water authority for supplying the existing relevant data. The authors are grateful to the Dr. Thierry Alex Mara for kind help in improving the manuscript.

References

- Abdulshahed AM, Longstaff AP, Fletcher S (2015) The application of ANFIS prediction models for thermal error compensation on CNC machine tools. *Appl Soft Comput* 27:158–168. doi:[10.1016/j.asoc.2014.11.012](https://doi.org/10.1016/j.asoc.2014.11.012)
- Adamowski JF (2008) Development of a short-term river flood forecasting method for snowmelt driven floods based on wavelet and cross-wavelet analysis. *J Hydrol* 353(3–4):247–266. doi:[10.1016/j.jhydrol.2008.02.013](https://doi.org/10.1016/j.jhydrol.2008.02.013)
- Adamowski JF, Chan HG (2011) A wavelet neural network conjunction model for groundwater level forecasting. *J Hydrol* 407(1–4):28–40. doi:[10.1016/j.jhydrol.2011.06.013](https://doi.org/10.1016/j.jhydrol.2011.06.013)
- Adamowski JF, Sun K (2010) Development of a coupled wavelet transform and neural network method for flow forecasting of non-perennial rivers in semi-arid watersheds. *J Hydrol* 390(1–2):85–91. doi:[10.1016/j.jhydrol.2010.06.033](https://doi.org/10.1016/j.jhydrol.2010.06.033)
- Adamowski K, Prokoph A, Adamowski J (2009) Development of a new method of wavelet aided trend detection and estimation. *Hydrolog Process* 23:2686–2696
- Adamowski J, Adamowski K, Bougadis J (2010) Influence of trend on short duration design storms. *Water Resour Manage* 24:401–413
- Adamowski J, Prokoph A, Adamowski K (2012a) Influence of the 11 year solar cycle on annual streamflow maxima in Southern Canada. *J Hydrol* 442:55–62
- Adamowski J, Chan H, Prasher S, Sharda VN (2012b) Comparison of multivariate adaptive regression splines with coupled wavelet transform artificial neural networks for runoff forecasting in Himalayan micro-watersheds with limited data. *J Hydroinf* 3:731–744
- Ahuja N, Lertrattanapanich S, Bose NK (2005) Properties determining choice of mother wavelet. *IEEE Proc Image Signal Process* 152(5):659–664. doi:[10.1049/ip-vis:20045034](https://doi.org/10.1049/ip-vis:20045034)
- Akansu A, Haddad R (1992) Multi-resolution signal decomposition: transforms, wavelets. Academic Press Inc, Orlando
- Anctil F, Tape D (2004) An exploration of artificial neural network rainfall–runoff forecasting combined with wavelet decomposition. *J Environ Eng Sci* 3(Suppl.):S121–S128. doi:[10.1139/s03-071](https://doi.org/10.1139/s03-071)
- Araghi A, Adamowski J, Nalley D, Malard J (2015) Using wavelet transforms to estimate surface temperature trends and dominant periodicities in Iran based on gridded reanalysis data. *J Atmos Res* 11:52–72
- Asghri Moghaddam A, Allaf Najib M (2006) Hydrogeologic characteristics of the alluvial tuff aquifer of northern Sahand Mountain slopes, Tabriz, Iran. *Hydrogeol J* 14(7):1319–1329. doi:[10.1007/s10040-006-0036-1](https://doi.org/10.1007/s10040-006-0036-1)
- Aussem A, Campbell J, Murtagh F (1998) Wavelet-based feature extraction and decomposition strategies for financial forecasting. *J Comp Intel Fin*. 6(2):5–12
- Barzegar R (2014) The investigation of quantitative and qualitative of the Tabriz plain aquifer groundwater resources. MSc. Thesis. Dept. Natural Sciences, University of Tabriz
- Barzegar R, Asghari Moghaddam A, Kazemian N (2015a) Assessment of heavy metals concentrations with emphasis on arsenic in the Tabriz plain aquifers, Iran. *Environ Earth Sci* 74(1):297–313. doi:[10.1007/s12665-015-4123-2](https://doi.org/10.1007/s12665-015-4123-2)
- Barzegar R, Asghari Moghaddam A, Najib M, Kazemian N, Adamowski J (2015b) Characterization of hydrogeologic properties of the Tabriz plain multilayer aquifer system, NW Iran. *Arab J Geosci*. doi:[10.1007/s12517-015-2229-1](https://doi.org/10.1007/s12517-015-2229-1)
- Belayneh A, Adamowski J, Khalil B, Ozga-Zielinski B (2014) Long-term SPI drought forecasting in the Awash River Basin in Ethiopia using wavelet-support vector regression models. *J Hydrol* 508:418–429
- Borgonovo E, Plischke E (2015) Sensitivity analysis: a review of recent advances. *Eur J Oper Res* 248(3):869–887. doi:[10.1016/j.ejor.2015.06.032](https://doi.org/10.1016/j.ejor.2015.06.032)
- Butler C, Adamowski J (2015) Empowering marginalized communities in water resources management: addressing inequitable practices in Participatory Model Building. *J Environ Manag* 153:153–162
- Campisi S, Adamowski J, Oron G (2012) Forecasting urban water demand via wavelet-denoising and neural network models. Case study: city of Syracuse, Italy. *Water Resour Manag* 26:3539–3558

- Cannas B, Fanni A, See L, Sias G (2006) Data preprocessing for river flow forecasting using neural networks: wavelet transforms and data partitioning. *Phys Chem Earth* 31(18):1164–1171. doi:[10.1016/j.pce.2006.03.020](https://doi.org/10.1016/j.pce.2006.03.020)
- Chiu SL (1994) Fuzzy model identification based on cluster estimation. *J Intell Fuzz Sys* 2(3):267–278. doi:[10.3233/JIFS-1994-2306](https://doi.org/10.3233/JIFS-1994-2306)
- Cho KH, Sthiannopkao S, Pachepsky YA, Kim KW, Kim JH (2011) Prediction of contamination potential of groundwater arsenic in Cambodia, Laos, and Thailand using artificial neural network. *Water Res* 45(17):5535–5544. doi:[10.1016/j.watres.2011.08.010](https://doi.org/10.1016/j.watres.2011.08.010)
- Christopoulou EB, Skodras AN, Georgakilas AA (2002) The “A Trous” wavelet transform versus classical methods for the improvement of solar images. In: Proceedings of the 14th international conference on digital signal processing, vol 2, Santorini, Greece, 1–3, July 2002, pp 885–888
- Dawson CW, Wilby RL (2001) Hydrological modelling using artificial neural networks. *Prog Phys Geogr* 25(1):80–108. doi:[10.1177/030913330102500104](https://doi.org/10.1177/030913330102500104)
- De Giorgi MG, Congedo PM, Malvoni M, Laforgia D (2015) Error analysis of hybrid photovoltaic power forecasting models: a case study of mediterranean climate. *Energy Convers Manag* 100:117–130. doi:[10.1016/j.enconman.2015.04.078](https://doi.org/10.1016/j.enconman.2015.04.078)
- Einax JW, Aulinger A, Tumpling WV, Prange A (1999) Quantitative description of element concentrations in longitudinal river profiles by multiway PLS models. *Fresenius' J Anal Chem* 363(7):655–661. doi:[10.1007/s002160051267](https://doi.org/10.1007/s002160051267)
- Elhatip H, Kömür MA (2008) Evaluation of water quality parameters for the Mamasin dam in Aksaray City in the central Anatolian part of Turkey by means of artificial neural networks. *Environ Geol* 53(6):1157–1164. doi:[10.1007/s00254-007-0705-y](https://doi.org/10.1007/s00254-007-0705-y)
- Emamgholizadeh S, Kashi H, Marofpoor I, Zalaghi E (2014) Prediction of water quality parameters of Karoon River (Iran) by artificial intelligence-based models. *Int J Environ Sci Tech* 11(3):645–656. doi:[10.1007/s13762-013-0378-x](https://doi.org/10.1007/s13762-013-0378-x)
- Fijani E, Nadiri AA, Asghari Moghaddam A, Tsai F, Dixon B (2013) Optimization of DRASTIC method by supervised committee machine artificial intelligence to assess groundwater vulnerability for Maragheh-Bonab Plain Aquifer, Iran. *J Hydrol* 503:89–100. doi:[10.1016/j.jhydrol.2013.08.038](https://doi.org/10.1016/j.jhydrol.2013.08.038)
- Ghavidel SZ, Montaseri M (2014) Application of different data-driven methods for the prediction of total dissolved solids in the Zarinehroud basin. *Stoch Environ Res Risk Assess* 28(8):2101–2118. doi:[10.1007/s00477-014-0899-y](https://doi.org/10.1007/s00477-014-0899-y)
- Govindaraju RS (2000) Artificial neural networks in hydrology. I, preliminary concepts. *J Hydrol Eng* 5(2):115–123. doi:[10.1061/\(ASCE\)1084-0699\(2000\)5:2\(115\)](https://doi.org/10.1061/(ASCE)1084-0699(2000)5:2(115)
- Grossmann A, Morlet J (1984) Decomposition of Hardy function into square integrable wavelets of constant shape. *J Math Anal* 5:723–736. doi:[10.1137/0515056](https://doi.org/10.1137/0515056)
- Hadad K, Pourahmadi M, Majidi-Maraghi H (2011) Fault diagnosis and classification based on wavelet transform and neural network. *Prog Nucl Energy* 53(1):41–47. doi:[10.1016/j.pnucene.2010.09.006](https://doi.org/10.1016/j.pnucene.2010.09.006)
- Haidary A, Amiri BJ, Adamowski J, Fohrer N, Nakane K (2013) Assessing the impacts of four land use types on the water quality of wetlands in Japan. *Water Resour Manag* 27:2217–2229
- Halbe J, Pahl-Wostl C, Sendzimir J, Adamowski J (2013) Towards adaptive and integrated management paradigms to meet the challenges of water governance. *Water Sci Technol* 67:2651–2660
- Halbe J, Adamowski J, Bennett E, Pahl-Wostl C, Farahbakhsh K (2014) Functional organization analysis for the design of sustainable engineering systems. *Ecol Eng* 73:80–91
- Hernández E, Weiss G (1996) A First Course on Wavelets. CRC Press, Boca Raton
- Inam A, Adamowski J, Halbe J, Prasher S (2015) Using causal loop diagrams for the initialization of stakeholder engagement in soil salinity management in agricultural watersheds in developing countries: a case study in the Rechna Doab watershed, Pakistan. *J Environ Manag* 152:251–267
- Jain A, Indurthy SKVP (2003) Comparative analysis of event based rainfall runoff modeling techniques-deterministic, statistical, and artificial neural networks. *J Hydraul Eng* 8:93–98. doi:[10.1061/\(ASCE\)1084-0699\(2003\)8:2\(93\)](https://doi.org/10.1061/(ASCE)1084-0699(2003)8:2(93)
- Jang JSR (1993) ANFIS: adaptive network based fuzzy inference system. *IEEE Trans Syst Man Cybern* 23(3):665–685. doi:[10.1109/21.256541](https://doi.org/10.1109/21.256541)
- Junsawang P, Asavant J, Lursinsap C (2007) Artificial Neural Network Model for Rainfall-Runoff Relationship, ASIMMOD, Chiang Mai, Thailand. http://www.mcc.cmu.ac.th/ASIMMOD2007/Paper/C07_P.%20Junsawang.pdf. Accessed 31 Dec 2015
- Kant A, Suman PK, Giri BK, Tiwari MK, Chatterjee C, Nayak PC, Kumar S (2013) Comparison of multi-objective evolutionary neural network, adaptive neuro-fuzzy inference system and bootstrap-based neural network for flood forecasting. *Neural Comput Appl* 23:231–246. doi:[10.1007/s00521-013-1344-8](https://doi.org/10.1007/s00521-013-1344-8)
- Karran D, Morin E, Adamowski J (2014) Multi-step streamflow forecasting using data-driven non-linear methods in contrasting climate regimes. *J Hydroinf* 16(3):671–689
- Kirchgässner G, Wolters J, Hassler U (2013) Introduction to modern time series analysis, 2nd edn. Springer, Berlin, p 331
- Kişi O (2008) Stream flow forecasting using neuro-wavelet technique. *Hydrolog Proc* 22(20):4142–4152. doi:[10.1002/hyp.7014](https://doi.org/10.1002/hyp.7014)
- Kişi O, Shiri J (2012) Reply to discussion of Precipitation forecasting using wavelet-genetic programming and wavelet-neuro-fuzzy conjunction models. *Water Resour Manag* 26(12):3663–3665. doi:[10.1007/s11269-012-0060-y](https://doi.org/10.1007/s11269-012-0060-y)
- Kolinjivadi V, Adamowski J, Kosoy N (2014) Recasting payments for ecosystem services (PES) in water resource management: a novel institutional approach. *Ecosyst Serv* 10:144–154
- Lau KM, Weng H (1995) Climate signal detection using wavelet transform: how to make a time series sing. *Bull Am Meteorol Soc* 76(12):2391–2402. doi:[10.1175/1520-477\(1995\)076<2391:CSDUWT>2.0.CO;2](https://doi.org/10.1175/1520-477(1995)076<2391:CSDUWT>2.0.CO;2)
- Maheswaran R, Khosa R (2012a) Comparative study of different wavelets for hydrologic forecasting. *Comput Geosci* 46:284–295. doi:[10.1016/j.cageo.2011.12.015](https://doi.org/10.1016/j.cageo.2011.12.015)
- Maheswaran R, Khosa R (2012b) Wavelet-Volterra coupled model for monthly stream flow forecasting. *J Hydrol* 450–451:320–335. doi:[10.1016/j.jhydrol.2012.04.017](https://doi.org/10.1016/j.jhydrol.2012.04.017)
- Maier HR, Dandy GC (2000) Neural networks for the prediction and forecasting of water resources variables: a review of modelling issues and applications. *Environ Model Softw* 15(1):101–124. doi:[10.1016/S1364-8152\(99\)00007-9](https://doi.org/10.1016/S1364-8152(99)00007-9)
- Mallat SG (1998) A wavelet tour of signal processing, 2nd edn. Academic Press, San Diego
- Mehrotra K, Mohan CK, Ranka S (1997) Elements of artificial neural networks. The MIT Press, Boston
- Mishra AK, Desai VR (2006) Drought forecasting using feed-forward recursive neural network. *Ecol Model* 198(1–2):127–138. doi:[10.1016/j.ecolmodel.2006.04.017](https://doi.org/10.1016/j.ecolmodel.2006.04.017)
- Moosavi V, Vafakhah M, Shirzohmehmadi B, Behnia N (2013) A wavelet-ANFIS hybrid model for groundwater level forecasting for different prediction periods. *Water Resour Manag* 27(5):1301–1321. doi:[10.1007/s11269-012-0239-2](https://doi.org/10.1007/s11269-012-0239-2)
- Najah AA, El-Shafie A, Karim OA, Jaafar O (2011) Integrated versus isolated scenario for prediction dissolved oxygen at progression of water quality monitoring stations. *Hydrolog Earth Syst Sci* 15:2693–2708. doi:[10.5194/hess-15-2693-2011](https://doi.org/10.5194/hess-15-2693-2011)

- Najah AA, El-Shafie A, Karim OA, Jaafar O (2012) Water quality prediction model utilizing integrated wavelet-ANFIS model with cross-validation. *Neural Comput Appl* 21(5):833–841. doi:[10.1007/s00521-010-0486-1](https://doi.org/10.1007/s00521-010-0486-1)
- Najah A, El-Shafie A, Karim OA, El-Shafie AH (2013) Application of artificial neural networks for water quality prediction. *Neural Comput Appl* 22(1, Suppl.):187–201. doi:[10.1007/s00521-012-0940-3](https://doi.org/10.1007/s00521-012-0940-3)
- Najah A, El-Shafie A, Karim OA, El-Shafie AH (2014) Performance of ANFIS versus MLP-NN dissolved oxygen prediction models in water quality monitoring. *Environ Sci Pollut Res* 21(3):1658–1670. doi:[10.1007/s11356-013-2048-4](https://doi.org/10.1007/s11356-013-2048-4)
- Nalley D, Adamowski JF, Khalil B (2012) Using discrete wavelet transforms to analyze trends in streamflow and precipitation in Quebec and Ontario (1954–2008). *J Hydrol* 475:204–228. doi:[10.1016/j.jhydrol.2012.09.049](https://doi.org/10.1016/j.jhydrol.2012.09.049)
- Nalley D, Adamowski JF, Khalil B, Ozga-Zielinski B (2013) Trend detection in surface air temperature in Ontario and Quebec, Canada during 1967–2006 using the discrete wavelet transform. *Atmos Res* 132–133:375–398. doi:[10.1016/j.atmosres.2013.06.011](https://doi.org/10.1016/j.atmosres.2013.06.011)
- Nayak PC, Sudheer KP, Ranjan DM, Ramasastry KS (2004) A neuro fuzzy computing technique for modeling hydrological time series. *J Hydrol* 291:52–66. doi:[10.1016/j.jhydrol.2003.12.010](https://doi.org/10.1016/j.jhydrol.2003.12.010)
- Nievergelt Y (2001) Wavelets made easy. Birkhäuser, Boston
- Noori R, Abdoli MA, Farokhnia A, Abbasi M (2009) Results uncertainty of solid waste generation forecasting by hybrid of wavelet transform-ANFIS and wavelet transform-neural network. *Expert Syst Appl* 36(6):9991–9999. doi:[10.1016/j.eswa.2008.12.035](https://doi.org/10.1016/j.eswa.2008.12.035)
- Nourani V, Alami MT, Aminfar MH (2009) A combined neural-wavelet model for prediction of watershed precipitation, Lighvanchai, Iran. *Eng Appl Artif Intell* 22(3):466–472. doi:[10.1016/j.engappai.2008.09.003](https://doi.org/10.1016/j.engappai.2008.09.003)
- Nourani V, Kisi Z, Mehdi K (2011) Two hybrid artificial Intelligence approaches for modeling rainfall-runoff process. *J Hydrol* 402(1–2):41–59. doi:[10.1016/j.jhydrol.2011.03.002](https://doi.org/10.1016/j.jhydrol.2011.03.002)
- Nourani V, Hosseini Baghanam A, Adamowski J, Gebremichael M (2013) Using self-organizing maps and wavelet transforms for space-time pre-processing of satellite precipitation and runoff data in neural network based rainfall-runoff modeling. *J Hydrol* 476:228–243. doi:[10.1016/j.jhydrol.2012.10.054](https://doi.org/10.1016/j.jhydrol.2012.10.054)
- Nourani V, Hosseini Baghanam A, Adamowski J, Kisi O (2014) Applications of hybrid Wavelet-Artificial Intelligence models in hydrology: a review. *J Hydrol* 514:358–377. doi:[10.1016/j.jhydrol.2014.03.057](https://doi.org/10.1016/j.jhydrol.2014.03.057)
- Olkonen H (2011) Discrete wavelet transform-biomedical application. InTech, Rijeka. doi:[10.5772/1818](https://doi.org/10.5772/1818)
- Palani S, Lioung SY, Tkalich P (2008) An ANN application for water quality forecasting. *Marine Pollut Bull* 56(9):1586–1597. doi:[10.1016/j.marpolbul.2008.05.021](https://doi.org/10.1016/j.marpolbul.2008.05.021)
- Parmar KS, Bhardwaj R (2015) River water prediction modeling using neural networks, fuzzy and wavelet coupled model. *Water Resour Manag* 29(1):17–33. doi:[10.1007/s11269-014-0824-7](https://doi.org/10.1007/s11269-014-0824-7)
- Partal T, Kişi Ö (2007) Wavelet and neuro fuzzy conjunction model for precipitation forecasting. *J Hydrol* 342:199–212. doi:[10.1016/j.jhydrol.2007.05.026](https://doi.org/10.1016/j.jhydrol.2007.05.026)
- Percival DB, Walden AT (2000) Wavelet methods for time series analysis. Cambridge University Press, New York
- Pingale S, Khare D, Jat M, Adamowski J (2014) Spatial and temporal trends of mean and extreme rainfall and temperature for the 33 urban centres of the arid and semi-arid state of Rajasthan, India. *J Atmos Res* 138:73–90
- Rahimikhoob A (2010) Estimation of evapotranspiration based on only air temperature data using artificial neural networks for a subtropical climate in Iran. *Theor Appl Climatol* 101(1–2):83–91. doi:[10.1007/s00704-009-0204-z](https://doi.org/10.1007/s00704-009-0204-z)
- Rajaee T, Mirbagheri SA, Zounemat-Kermani M, Nourani V (2009) Daily suspended sediment concentration simulation using ANN and neuro-fuzzy models. *Sci Total Environ* 407(17):4916–4927. doi:[10.1016/j.scitotenv.2009.05.016](https://doi.org/10.1016/j.scitotenv.2009.05.016)
- Rathinasamy M, Adamowski JF, Khosa R (2013) Multiscale streamflow forecasting using a new Bayesian Model Average based ensemble multi-wavelet Volterra nonlinear method. *J Hydrol* 507:186–200. doi:[10.1016/j.jhydrol.2013.09.025](https://doi.org/10.1016/j.jhydrol.2013.09.025)
- Rathinasamy M, Khosa R, Adamowski J, Ch S, Partheepan G, Anand J, Narsimlu B (2015) Wavelet-based multiscale performance analysis: an approach to assess and improve hydrological models. *Water Resour Res*. doi:[10.1002/2013WR014650](https://doi.org/10.1002/2013WR014650)
- Ravansalar M, Rajaee T (2015) Evaluation of wavelet performance via an ANN-based electrical conductivity prediction model. *Environ Monit Assess*. doi:[10.1007/s10661-015-4590-7](https://doi.org/10.1007/s10661-015-4590-7)
- Saadat H, Adamowski J, Bonnell R, Sharifi F, Namdar M, Ale-Ebrahim S (2011) Land use and land cover classification over a large area in Iran based on single date analysis of satellite imagery. *J Photogramm Remote Sens* 66(5):608–619
- Sehgal V, Tiwari MK, Chatterjee C (2014) Wavelet bootstrap multiple linear regression based hybrid modeling for daily river discharge forecasting. *Water Resour Manag* 28(10):2793–2811. doi:[10.1007/s11269-014-0638-7](https://doi.org/10.1007/s11269-014-0638-7)
- Shirmohammadi B, Vafakhah M, Moosavi V, Moghaddamnia A (2013) Application of several data-driven techniques for predicting groundwater level. *Water Resour Manag* 27(2):419–432. doi:[10.1007/s11269-012-0194-y](https://doi.org/10.1007/s11269-012-0194-y)
- Singh KP, Basant A, Malik A, Jain G (2009) Artificial neural network modeling of the river water quality, a case study. *Ecol Model* 220(6):888–895. doi:[10.1016/j.ecolmodel.2009.01.004](https://doi.org/10.1016/j.ecolmodel.2009.01.004)
- Smith M (1994) Neural networks for statistical modelling. Van Nostrand Reinhold, New York, p 235
- Strait D, Adamowski J, Reilly K (2014) Exploring the attributes, strategies and contextual knowledge of champions of change in the Canadian water sector. *Can Water Resour J* 39(3):255–269
- Tiwari M, Adamowski J (2014) Urban water demand forecasting and uncertainty assessment using ensemble wavelet-bootstrap-neural network models. *Water Resour Res* 49(10):6486–6507
- Tiwari M, Adamowski J (2015) Medium-term urban water demand forecasting with limited data using an ensemble wavelet-bootstrap machine-learning approach. *J Water Resour Plan Manag* 141(2):04014053
- Tiwari M, Chatterjee C (2011) new wavelet–bootstrap–ANN hybrid model for daily discharge forecasting. *J Hydroinf* 13(3):500–519. doi:[10.2166/hydro.2010.142](https://doi.org/10.2166/hydro.2010.142)
- Torrance C, Compo GP (1998) A practical guide to wavelet analysis. *Bull Am Meteorol Soc* 79:61–78. doi:[10.1175/1520-0477\(1998\)079<061:APGTWA>2.0.CO;2](https://doi.org/10.1175/1520-0477(1998)079<061:APGTWA>2.0.CO;2)
- Xu L, Liu S (2013) Study of short-term water quality prediction model based on wavelet neural network. *Math Comput Model* 58(3–4):807–813. doi:[10.1016/j.mcm.2012.12.023](https://doi.org/10.1016/j.mcm.2012.12.023)
- Yeniguna K, Ecer R (2012) Overlay mapping trend analysis technique and its application in Euphrates Basin, Turkey. *Meteorol Appl* 20(4):427–438. doi:[10.1002/met.1304](https://doi.org/10.1002/met.1304)
- Zounemat-Kermani M, Teshnehlab M (2008) Using adaptive neuro-fuzzy inference system for hydrological time series prediction. *Appl Soft Comput* 8(2):928–936. doi:[10.1016/j.asoc.2007.07.011](https://doi.org/10.1016/j.asoc.2007.07.011)